AD-A081 862 NAVAL UNDERWATER SYSTEMS CENTER NEWPORT RI F/G 20/4
AN OPTIMAL DEPTH CONTROL TECHNIQUE FOR UNDERWATER VEHICLES.(U)
SEP 79 J J PERRUZZI
UNCLASSIFIED NUSC-TR-5440 NL

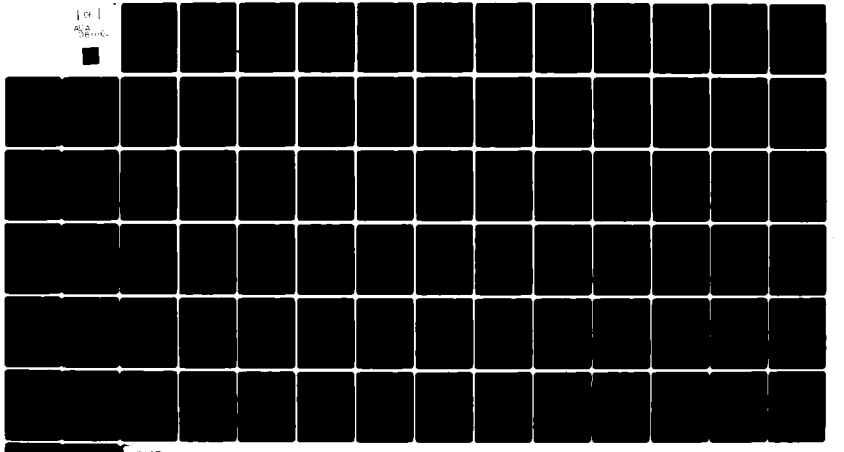

END
DATE FILMED
4-80
DTIC

NUSC Technical Report 5440
15 September 1979

# An Optimal Depth Control Technique for Underwater Vehicles

Joseph J. Perruzzi
Combat Control Systems Department





Naval Underwater Systems Center
Newport, Rhode Island 02840

## PREFACE

This project was conducted as part of the Naval Underwater Systems Center's program of independent research; NUSC Project No. A45321, "Optimal Controllers for Underwater Vehicles" (principal investigator, Joseph J. Perruzzi, NUSC Code 3522) and under Navy Subproject and Task No. ZR-000-0101/61152N. The sponsoring activity is the Naval Material Command (program manager, J. H. Probus, Code MAT-08T1).

This report was presented to the faculty of the School of Electrical Engineering at Southeastern Massachusetts University in partial fulfillment of the requirements for the degree of Master of Science in Electrical Engineering.

The technical reviewer for this report was Professor Daniel J. Murphy, Professor of Electrical Engineering at Southeastern Massachusetts University and consultant to NUSC Code 3522.

## ACKNOWLEDGMENTS

The author thanks Professor Daniel J. Murphy for his ideas and guidance throughout this research and Kathy Perruzzi for her patience in typing the initial draft of this document.

REVIEWED AND APPROVED: 15 September 1979

W. A. Von Winkle

W. A. Von Winkle
Associate Technical Director for Technology

(14) NUSC — REPORT DOCUMENTATION PAGE

READ INSTRUCTIONS BEFORE COMPLETING FORM

| 1. REPORT NUMBER | 2. GOVT ACCESSION NO. | 3. RECIPIENT'S CATALOG NUMBER |
|---|---|---|
| TR-5448 | (9) | Technical Rept. |

4. TITLE (and Subtitle)

(6) AN OPTIMAL DEPTH CONTROL TECHNIQUE FOR UNDERWATER VEHICLES

5. TYPE OF REPORT & PERIOD COVERED

6. PERFORMING ORG. REPORT NUMBER

7. AUTHOR(s)

(10) Joseph J. Perruzzi

8. CONTRACT OR GRANT NUMBER(s)

9. PERFORMING ORGANIZATION NAME AND ADDRESS

Naval Underwater Systems Center
Newport Laboratory
Newport, Rhode Island 02840

10. PROGRAM ELEMENT, PROJECT, TASK AREA & WORK UNIT NUMBERS

NUSC Project No. A45321
Subproject/Task No.
ZR-000-0101/61152N

11. CONTROLLING OFFICE NAME AND ADDRESS

Chief of Naval Material (MAT-08T1)
Navy Department
Washington, D.C. 20360

(11)

12. REPORT DATE

15 Sep[illegible] 1979

13. NUMBER OF PAGES

84

14. MONITORING AGENCY NAME & ADDRESS(if different from Controlling Office)

(16) ZK0000[illegible]

15. SECURITY CLASS. (of this report)

UNCLASSIFIED (12) 84

15a. DECLASSIFICATION/DOWNGRADING SCHEDULE

16. DISTRIBUTION STATEMENT (of this Report)

DISTRIBUTION STATEMENT A
Approved for public release;
Distribution Unlimited

(17) ZR000C1[illegible]

17. DISTRIBUTION STATEMENT (of the abstract entered in Block 20, if different from Report)

Approved for public release; distribution unlimited.

18. SUPPLEMENTARY NOTES

19. KEY WORDS (Continue on reverse side if necessary and identify by block number)

Torpedo Control Techniques
Optimal Control Theory

20. ABSTRACT (Continue on reverse side if necessary and identify by block number)

This report develops a general control technique, based on modern control theory, which maintains an underwater vehicle such as a torpedo at a constant depth. A state variable mathematical model of an underwater vehicle in conjunction with a quadratic cost functional were used to determine the optimal control technique. Included in the model are the effects of a non-neutrally buoyant vehicle with different centers of gravity and buoyancy, and the effects of ocean currents when the vehicle is operating near the surface in

DD FORM 1 JAN 73 1473

406 267

20. ABSTRACT (Cont'd)

high sea state conditions. Three of the state variables are directly observable, but the fourth state must be estimated using a reduced-order Luenberger observer. Once all the states become available, the optimal control problem is formulated as an output regulator with a constant reference input vector. The results of torpedo simulations illustrating the feasibility of the closed-loop control scheme are presented and discussed.

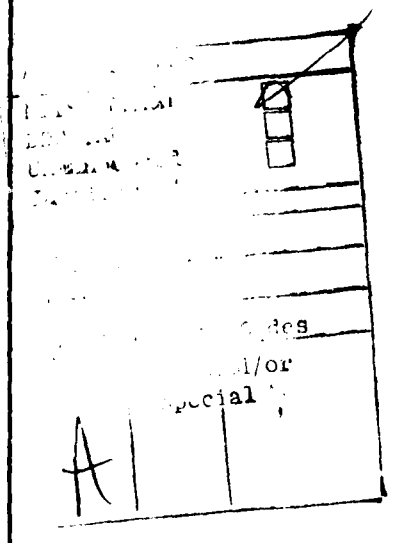

TABLE OF CONTENTS

# LIST OF ILLUSTRATIONS

## LIST OF ILLUSTRATIONS (Cont'd)



## LIST OF TABLES

# AN OPTIMAL DEPTH CONTROL TECHNIQUE FOR UNDERWATER VEHICLES

## SECTION I
## INTRODUCTION

The ability of a torpedo or a torpedo-like vehicle to maintain a preset depth and course is a fundamental prerequisite for successful operation. This is equally true whether the vehicle is operating in a calm sea devoid of all currents, or in high sea state conditions near the surface where it would likely be very much affected by ocean currents and wave induced eddies. In addition, most torpedo-like underwater vehicles are non-neutrally buoyant and have centers of gravity and buoyancy that do not coincide. For such vehicles to maintain a constant depth, the steady state values for pitch angle, angle of attack, and elevator deflection have non-zero values (reference 1).

The approach used here to develop an optimal depth control law for torpedoes is applicable to underwater vehicles in general, and the technique developed will maintain a vehicle at a constant depth when it operates under the influence of seaway disturbances and weight-buoyancy imbalances. The hydrodynamic equations of motion for a symmetrical underwater vehicle are used in the development of state feedback controllers for such vehicles. In the past, development of these closed-loop controllers was accomplished by using either a classical approach (references 2, 3, 4) or by computer simulations (references 5 - 6). This report analytically derives the feedback gains utilizing modern control theory and Luenberger observer theory (reference 7). Emphasis is focused on

such factors as the realization of a linear state variable model, in which the states are completely controllable and observable, and a performance index which weights the tradeoffs between errors in vehicle depth and expenditure of control effort to correct these depth errors.

In Section II a linear, controllable, and observable state variable model of the pitch plane dynamics of the vehicle is developed in terms of the hydrodynamic moments and forces given in reference 8. A differential equation delineating the vertical velocity of the vehicle is included in this model, which is for a non-neutrally buoyant vehicle with different centers of gravity and buoyancy, and which takes into account the effects of ocean disturbances. The state variables sufficient to define this system are vehicle depth, pitch, pitch rate, and angle of attack (resulting in a fourth-order system). Three of the state variables are available for measurement at the output, but the fourth state, angle of attack, must be estimated by using a reduced order Luenberger observer.

In Section III, the optimal control problem is formulated as an output regulator with a constant reference input vector (reference 1). This approach determines an optimal control law that keeps the output of the dynamic system near a constant reference while minimizing a quadratic cost functional. The quadratic cost functional comprises a weighted error state vector (the difference between the output of the dynamic model and a desired constant input) and a weighted input state vector. Minimization of the quadratic cost functional results in an optimal control law, which drives the output to the desired reference while min-

imizing control expended. The resulting control law is the product of the states of the system and a constant gain matrix, which is a function of the weighting matrices in the cost functional and the linear state variable model. The development of a reduced-order Luenberger observer to obtain an estimate of the angle of attack is included.

The hydrodynamic coefficients of a typical torpedo traveling at a constant speed are used in the state variable model to illustrate the feasibility of the control scheme. The model was simulated on a digital computer and the stability of the vehicle is analyzed for different performance index weighting matrices and vehicle speeds. The optimal control law was formulated for a linear state variable model, but limitations were placed on both the vehicle's pitch and rudder deflection in the simulation. By adjusting the weighting matrices in the performance index, a good solution to the nonlinear problem can be obtained. Also, since the closed-loop transfer function is stable, the control scheme will enter the linear range. Calcomp plots of the states and control inputs were made to aid in the analysis of the optimal controller developed herein. These are presented and discussed in Section IV.

# SECTION II

# DEVELOPMENT OF THE STATE VARIABLE MODEL

From the hydrodynamic equations of motion of an underwater vehicle, a linear, controllable, and observable state variable model is developed that takes into account the effects of seaway disturbances. This model is simplified by assuming that the vehicle is neutrally buoyant with centers of gravity and buoyancy that coincide, and also that the vehicle is not affected by seaway disturbances. This simplified model is used to develop the initial optimal control law presented in the next section.

## LINEAR PITCH PLANE MODEL

The equations of motion for a submerged hydrodynamic body in the yaw, pitch, and roll planes are given in reference 8. To simplify these equations, the following assumptions are made (from reference 2).

1. Pitch, yaw, and angle of attack satisfy the small angle approximations.
2. Vehicle is traveling at a constant speed.
3. Roll motion is constrained to negligibly small values by the roll control system.

Under these conditions, the roll, yaw, and pitch dynamics are mutually decoupled. This results in a set of linear equations that represents the force and moment summations. Figure 1 depicts a submerged vehicle in the pitch plane.

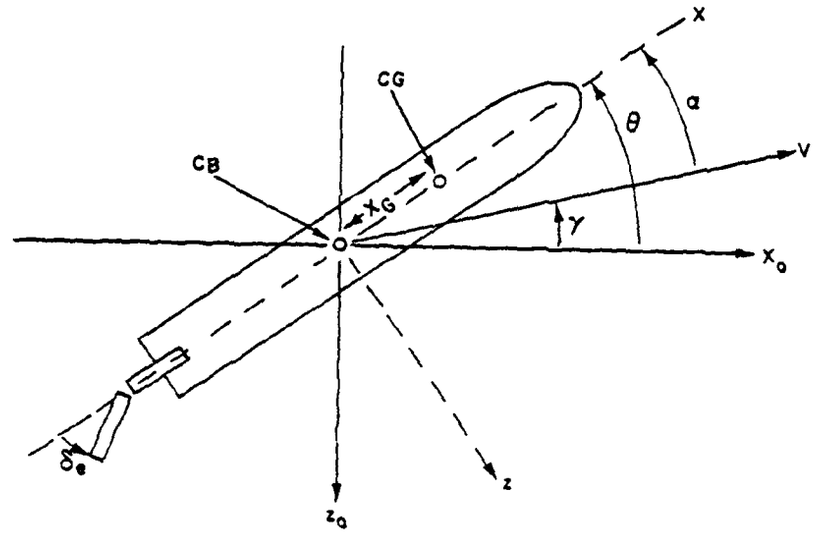


Figure 1. Submerged Vehicle in the Pitch Plane

The linear pitch plane equations are

$$m_t V\dot{\alpha} = mX_g\ddot{\theta} + (Z_q + m_L V)\dot{\theta} + Z_\alpha\alpha + Z_{\delta e}\delta_e + (W-B) \quad * \tag{1}$$

and

$$J_y\ddot{\theta} = mX_g V\dot{\alpha} + M_\alpha\alpha + (M_q - mX_g V)\dot{\theta} + M_{\delta e}\delta_e - WX_g \tag{2}$$

where

$\alpha$ ≡ angle of attack

$\theta$ ≡ pitch angle

$\delta_e$ ≡ elevator deflection

and the vehicle constants and the hydrodynamic coefficients are defined in appendix A.

---

* ($\dot{}$) indicates $\frac{d}{dt}(\ )$ and ($\ddot{}$) indicates $\frac{d^2}{dt^2}(\ )$

The depth equation is given by

$$\dot{Z}_o = -V\sin(\theta-\alpha) \approx -V(\theta-\alpha) \tag{3}$$

where

$Z_o \equiv$ depth of vehicle below the mean surface.

STATE VARIABLE REPRESENTATION

Equations (1), (2), and (3) are put into a state variable notation by letting

$$\begin{aligned} X_1(t) &= Z_o \\ X_2(t) &= \vartheta \\ X_3(t) &= \dot{\theta} = \dot{X}_2(t) \\ X_4(t) &= \alpha \\ \text{and } \mu(t) &= \delta_e \end{aligned} \tag{4}$$

In terms of the state variables defined, the state equations are written directly from equations (1), (2), and (3) as

$$m_t V\dot{X}_4(t) = mX_g\dot{X}_3(t) + (Z_q+m_L V)X_3(t) + Z_\alpha X_4(t) + Z_{\delta e}U(t) + (W-B) \tag{5}$$

$$J_y\dot{X}_3(t) = mX_g V\dot{X}_4(t) + M_\alpha X_4(t) + (M_q-mX_g V)X_3(t) + M_{\delta e}U(t) - WX_g \tag{6}$$

$$\dot{X}_1(t) = -VX_2(t) + VX_4(t). \tag{7}$$

Solving for the states $\dot{X}_3(t)$ and $\dot{X}_4(t)$ in equations (5) and (6) and using equations (4) and (7) results in a state variable representation of the form

$$\dot{X}_1(t) = -VX_2(t) + VX_4(t) \tag{8a}$$

$$\dot{X}_2(t) = X_3(t) \tag{8b}$$

$$\dot{X}_3(t) = \bar{a}_1 X_3(t) + \bar{a}_2 X_4(t) + \bar{b}_1 U(t) + \bar{b}_3 \tag{8c}$$

$$\dot{X}_4(t) = \bar{a}_3 X_3(t) + \bar{a}_4 X_4(t) + \bar{b}_2 U(t) + \bar{b}_4 \tag{8d}$$

where

$$\bar{a}_1 = \frac{[mX_g(Z_q+m_L V)+(M_q-mX_g V)m_t]}{\beta} \tag{8e}$$

$$\bar{a}_2 = \frac{[mX_g Z_\alpha + M_\alpha m_t]}{\beta} \tag{8f}$$

$$\bar{a}_3 = \frac{Jy[Z_q+m_L V] + mX_g[M_q-mX_g V]}{V\beta} \tag{8g}$$

$$\bar{a}_4 = \frac{Jy\ Z_\alpha + mX_g M_\alpha}{V\beta} \tag{8h}$$

$$\bar{b}_1 = \frac{mX_g Z_{\delta e} + m_t M_{\delta e}}{\beta} \tag{8i}$$

$$\bar{b}_2 = \frac{Jy\ Z_{\delta e} + mX_g M_{\delta e}}{V\beta} \tag{8j}$$

$$\bar{b}_3 = \frac{[mX_g(W-B) - WX_g m_t]}{\beta} \tag{8k}$$

$$\bar{b}_4 = \frac{Jy(W-B) - mX_g^2 W}{V\beta} \tag{8l}$$

and

$$\beta = J_y m_t - m^2 X_g^2. \tag{8m}$$

SEAWAY DISTURBANCE ON UNDERWATER VEHICLE OPERATION

When an underwater vehicle operates near the surface in a high sea state condition, ocean currents can cause the vehicle to deviate from the desired trajectory. To include the effect of such seaway disturbances, the following assumptions are made (reference 2).

1. The dynamic response to control surface deflection is independent of the disturbance effects.
2. The horizontal speed, in relation to an inertial axis, is relatively unaffected by water particle velocity and vehicle maneuvering.
3. The vehicle is sufficiently thin so that there is no dynamic pressure difference between the vehicle top and bottom.
4. The vehicle length is short compared to the wavelength of the waves of interest.

These assumptions reduce the seaway disturbances to the vertical velocity of the water particles, $V_w$, which results in the addition of a force and moment component to equations (5) and (6), respectively. Equations (5) and (6) become

$$m_t V\dot{X}_4(t) = mX_g\dot{X}_3(t) + (Z_q + m_L V)X_3(t) + Z_\alpha X_4(t) + Z_{\delta e}U(t) + (W-B) - Z_w V_w \tag{9}$$

$$J_y\dot{X}_3(t) = mX_g VX_4(t) + M_\alpha\dot{X}_4(t) + (M_q - mX_g V)X_3(t) + M_{\delta e}\,U(t) - WX_g - M_w V_w \tag{10}$$

and the state variable model is modified to yield

$$\dot{X}_1(t) = -VX_2(t) + VX_4(t) \tag{11a}$$

$$\dot{X}_2(t) = X_3(t) \tag{11b}$$

$$\dot{X}_3(t) = \bar{a}_1X_3(t) + \bar{a}_2X_4(t) + \bar{b}_1\,U(t) + \bar{d}_1 \tag{11c}$$

$$\dot{X}_4(t) = \bar{a}_3X_3(t) + \bar{a}_4X_4(t) + \bar{b}_2\,U(t) + \bar{d}_2 \tag{11d}$$

where

$$\bar{d}_1 = \bar{b}_3 - \frac{(mX_gZ_w + m_tM_w)}{\beta}\,V_w \tag{11e}$$

and

$$\bar{d}_2 = \bar{b}_4 - \frac{(J_yZ_w + mX_gM_w)}{V\beta}\,V_w \,. \tag{11f}$$

Comparing equations (8) and (11) shows that if the vertical water particle velocity is constant, the effect of the seaway disturbances is incorporated into the state veriable model as a constant bias.

The terms $\bar{d}_1$ and $\bar{d}_2$ in equations (11c) and (11d) are known constant biases due to the weight-buoyancy imbalance of the underwater vehicle, the different centers of gravity and buoyancy, and the seaway disturbance (reference 2). Equation (11) shows the steady state solution to be given by

$$X_2(t) = X_4(t) \tag{12}$$

$$X_3(t) = 0$$

$$\bar{a}_2 X_4(t) + \bar{b}_1 U(t) = -\bar{d}_1 \tag{13}$$

$$\bar{a}_4 X_4(t) + \bar{b}_2 U(t) = -\bar{d}_2. \tag{14}$$

From equations (13) and (14) it is seen that the state, angle of attack, and input control, U(t), have non-zero steady state values. Equation (12) shows that to maintain the vehicle at a constant depth, the pitch and angle of attack must be equal. More will be said about the effect of the known constant biases on the controller design in Section III.

The state variable representation may be written in matrix form as

$$\begin{bmatrix} \dot{X}_1(t) \\ \dot{X}_2(t) \\ \dot{X}_3(t) \\ \dot{X}_4(t) \end{bmatrix} = \begin{bmatrix} 0 & -V & 0 & V \\ 0 & 0 & 1 & 0 \\ 0 & 0 & \bar{a}_1 & \bar{a}_2 \\ 0 & 0 & \bar{a}_3 & \bar{a}_4 \end{bmatrix} \begin{bmatrix} X_1(t) \\ X_2(t) \\ X_3(t) \\ X_4(t) \end{bmatrix} + \begin{bmatrix} 0 \\ 0 \\ \bar{b}_1 \\ \bar{b}_2 \end{bmatrix} U(t) + \begin{bmatrix} 0 \\ 0 \\ \bar{d}_1 \\ \bar{d}_2 \end{bmatrix}. \tag{15}$$

Equation (15) is written in a more compact form by letting

$$\bar{A} = \begin{bmatrix} 0 & -V & 0 & V \\ 0 & 0 & 1 & 0 \\ 0 & 0 & \bar{a}_1 & \bar{a}_2 \\ 0 & 0 & \bar{a}_3 & \bar{a}_4 \end{bmatrix}, \quad \underline{\bar{b}}^* = \begin{bmatrix} 0 \\ 0 \\ \bar{b}_1 \\ \bar{b}_2 \end{bmatrix}, \quad \underline{X}(t) = \begin{bmatrix} X_1(t) \\ X_2(t) \\ X_3(t) \\ X_4(t) \end{bmatrix}, \quad \underline{\bar{d}} = \begin{bmatrix} 0 \\ 0 \\ \bar{d}_1 \\ \bar{d}_2 \end{bmatrix}.$$

Using the above definition, the state variable model becomes

$$\dot{\underline{X}}(t) = \bar{A}\underline{X}(t) + \underline{\bar{b}}\, U(t) + \underline{\bar{d}}. \tag{16}$$

SIMPLIFIED STATE VARIABLE MODEL

The initial model to be used in developing the optimal controller assumes a neutrally buoyant vehicle with coincident centers of gravity and buoyancy and no seaway disturbances. With these assumptions, equation set (11) reduces to

$$\dot{X}_1(t) = -VX_2(t) + VX_4(t) \tag{17a}$$

$$\dot{X}_2(t) = X_3(t) \tag{17b}$$

$$\dot{X}_3(t) = a_1X_3(t) + a_2X_4(t) + b_1U(t) \tag{17c}$$

$$\dot{X}_4(t) = a_3X_3(t) + a_4X_4(t) + b_2U(t) \tag{17d}$$

---

* $(\dot{\cdot})$ indicates a vector quantity

where

$$a_1 = \frac{M_q}{J_y}$$

$$a_2 = \frac{M_\alpha}{J_y}$$

$$a_3 = \frac{Z_q + m_L V}{m_t V}$$

$$a_4 = \frac{Z_\alpha}{m_t V}$$

$$b_1 = \frac{M_{\delta e}}{J_y}$$

$$b_2 = \frac{Z_{\delta e}}{m_t V} .$$

Equation set (17) may be written as

$$\dot{\underline{X}}(t) = A\underline{X}(t) + \underline{b}U(t) \tag{18}$$

where

$$A = \begin{bmatrix} 0 & -V & 0 & V \\ 0 & 0 & 1 & 0 \\ 0 & 0 & a_1 & a_2 \\ 0 & 0 & a_3 & a_4 \end{bmatrix}, \quad \underline{b} = \begin{bmatrix} 0 \\ 0 \\ b_1 \\ b_2 \end{bmatrix}.$$

Once the optimal control law is formulated for the simplified state model given by equation (18), the control scheme will be modified to include the constant bias in equation set (11).

Since the states $X_1(t)$, $X_2(t)$, and $X_3(t)$ are available for measurement, the measurement equation is given by

$$\underline{M}(t) = C\underline{X}(t) + \underline{v}(t)$$

where

$$\underline{M}(t) = \begin{bmatrix} m_1(t) \\ m_2(t) \\ m_3(t) \end{bmatrix} \qquad C = \begin{bmatrix} 1 & 0 & 0 & 0 \\ 0 & 1 & 0 & 0 \\ 0 & 0 & 1 & 0 \end{bmatrix} \quad \text{and} \quad \underline{v}(t) = \begin{bmatrix} v_1(t) \\ v_2(t) \\ v_3(t) \end{bmatrix}$$

It will be assumed in this report that the measurement noise, $\underline{v}(t)$, is negligible. Thus, the measurement equation becomes

$$\underline{M}(t) = C\underline{X}(t). \tag{19}$$

A signal flow diagram of the state variable model given by equations (18) and (19) is shown in figure 2.

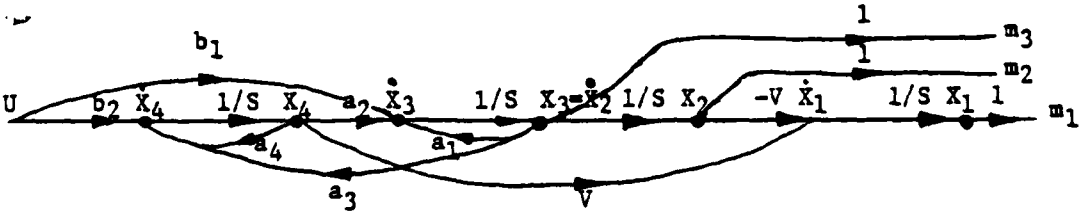


Figure 2. Signal Flow Graph of the State Variable Model

The controllability and observability of the state variable model given by equations (18) and (19) are shown in appendix B.

Thus far, a state variable model of the pitch plane dynamics of an underwater vehicle has been developed. This model was developed for a non-neutrally buoyant vehicle with different centers of gravity and buoyancy. Also accounted for in the model were the effects of seaway disturbances on the vehicle. This model was used to develop a simplified model, with assumptions being made that the vehicle is neutrally buoyant, has centers of gravity and buoyancy that coincide, and that there are no seaway disturbances to contend with. In the next section, an optimal control law is developed for both of these state variable models. Also included in the next section is the development of a Luenberger observer to make accessible the state component angle of attack, so that it can be used in the formulation of the optimal control law.

# SECTION III

# DEVELOPMENT OF THE CLOSED-LOOP CONTROL SYSTEM

In this section, the optimal control law is formulated for the simplified state variable model given by equations (18) and (19). A reduced-order Luenberger observer is also developed to obtain an estimate of the angle of attack. Once the control system is found for the simplified state variable model, it is modified to include the addition of the constant bias for the more-general state variable model given by equation set (11).

## FORMULATION OF THE OPTIMAL CONTROLLER: TRACKING PROBLEM

The optimal control law is found from the solution to the tracking problem. This solution leads to an optimal feedback system with the property that the output of the state variable model is kept near some constant while simultaneously minimizing a specified performance index. Following the precedure given in reference 1, a steady state solution to the tracking problem is found by redefining the state variable model so that the techniques employed in the solution to the output regulator problem are applicable. After formulating the optimal control law for the redefined model, the control law can be modified for the tracking problem.

The simplified linear state model of the pitch plane dynamics, from equation (18), is

$$\dot{\underline{X}}(t) = A\underline{X}(t) + \underline{b}U(t). \tag{20}$$

An output state equation that yields vehicle depth is given by

$$y(t) = \underline{c}'\underline{X}(t) \tag{21}$$

where

$\underline{c}' = [\ 1 \quad 0 \quad 0 \quad 0\ ]^*$ and $y(t) \equiv$ vehicle depth.

Defining a new set of state variables by letting

$$\hat{\underline{X}}(t) = \underline{X}(t) - \underline{X}_d \tag{22a}$$

$$\hat{y}(t) = y(t) - Z_d \tag{22b}$$

and

$$\hat{U}(t) = U(t) - U_d \tag{22c}$$

results in a redefined state variable model of the form

$$\dot{\hat{\underline{X}}}(t) = A\hat{\underline{X}}(t) + \underline{b}\hat{U}(t) \tag{23}$$

$$\hat{y}(t) = \underline{c}'\hat{\underline{X}}(t). \tag{24}$$

The terms $\underline{X}_d$, $Z_d$ and $U_d$ in equation (22) are:

$\underline{X}_d \equiv$ desired constant equilibrium state

$Z_d \equiv$ desired constant output

$U_d \equiv$ desired constant input.

More will be said about the above terms later.

---

* $(\cdot)'$ indicates the transpose of $(\cdot)$

The objective of the output regulator problem is to determine a control law by minimization of a quadratic performance index such that the output, $\hat{y}(t)$, remains near zero.

The performance index for the output regulator problem is defined as

$$J = \frac{1}{2} \int_0^\infty [\hat{y}'(t)Q\hat{y}(t) + \hat{U}'(t)R\hat{U}(t)]\, dt.$$

Reference 9 derives the optimal control law for the output regulator problem, and the result is

$$\hat{U}(t) = -R^{-1}\underline{b}'F\hat{\underline{X}}(t) = -K\hat{\underline{X}}(t) \tag{25a}$$

where the gains K are

$$K = [k_1 \quad k_2 \quad k_3 \quad k_4] \tag{25b}$$

and the matrix F,

$$F = \begin{bmatrix} f_{11} & f_{12} & f_{13} & f_{14} \\ f_{12} & f_{22} & f_{23} & f_{24} \\ f_{13} & f_{23} & f_{33} & f_{34} \\ f_{14} & f_{24} & f_{34} & f_{44} \end{bmatrix}, \tag{25c}$$

is the steady state solution to the matrix Riccati equation

$$FA + A'F - F\underline{b}R^{-1}\underline{b}'F + \underline{c}Q\underline{c}' = 0 \tag{26}$$

Substituting equation (25a) into equation (23) yields an optimal closed-loop system of the form

$$\dot{\hat{\underline{X}}}(t) = (A - \underline{b}K)\hat{\underline{X}}(t). \tag{27}$$

Even though the matrix A does not have to be stable, the system given by equation (27) is homogeneous and strictly stable, therefore

$$\lim_{t\to\infty} \hat{\underline{X}}(t) = 0 \tag{28a}$$

and from equation (24) it follows that

$$\lim_{t\to\infty} \hat{y}(t) = 0. \tag{28b}$$

Also, from (25a)

$$\lim_{t\to\infty} \hat{U}(t) = 0. \tag{28c}$$

Substituting the original system state variables given by equation set (22) into equation set (28) shows that

$$\lim_{t\to\infty} \underline{X}(t) = \underline{X}_d \tag{29a}$$

$$\lim_{t\to\infty} y(t) = Z_d \tag{29b}$$

and

$$\lim_{t\to\infty} U(t) = U_d. \tag{29c}$$

Condition (29b) implies that, in the steady state,

$$c'\underline{X}_d = Z_d \ . \tag{30}$$

Equation (30) is possible only if the optimal control law contains a constant bias, $U_d$, such that in the steady state

$$A\underline{X}_d + \underline{b}U_d = 0 \tag{31}$$

This is seen from equation (23) in the limit as $t\to\infty$.

Once equations (30) and (31) are formulated, the tracking problem can be solved as an output regulator problem by finding the control law that drives the output $\hat{y}(t)$ to zero. Using equation (25a) for $\hat{U}(t)$ while substituting the original state variables for the states $\hat{\underline{X}}(t)$ and $\hat{y}(t)$ into equations (23) and (24) shows that by maintaining the output $\hat{y}(t)$ near zero for the redefined state model, the output y(t) for the original state model is kept near the desired output, $Z_d$.

The optimal closed-loop system for the original state model becomes

$$\dot{\underline{X}}(t) = [A - \underline{b}K][\underline{X}(t) - \underline{X}_d] \tag{32}$$

$$y(t) = \underline{c}'\underline{X}(t) \tag{33}$$

The optimal control law for the original system is found by solving for the original control U(t) in equation (22c) while substituting the optimal control law given by equation (25a) for $\hat{U}(t)$.

The optimal control law becomes

$$U(t) = -K[\underline{X}(t) - \underline{X}_d] + U_d = -\hat{U}_o(t) + U_d \tag{34}$$

A closed-loop structure of the optimal control scheme is shown in figure 3, where double lines indicate the flow of vector quantities.

The optimal system can be represented in a different configuration by substituting from equation (31)

$$A\underline{X}_d = -\underline{b}U_d$$

into equation (32). The closed-loop system becomes

$$\dot{\underline{X}}(t) = [A-\underline{b}K]\underline{X}(t) + \underline{b}[U_d+K\underline{X}_d].$$

Let

$$r_d = U_d + K\underline{X}_d, \tag{35}$$

then the closed-loop system has the form

$$\dot{\underline{X}}(t) = [A - \underline{b}K]\underline{X}(t) + \underline{b}r_d .$$

The term $r_d$ is the desired reference signal for the optimal closed-loop system. The alternate configuration is shown in figure 4.

To put the tracking problem into a form equivalent to an output regulator problem, the desired output, $Z_d$, the equilibrium states, $\underline{X}_d$, and the biased input, $U_d$, must be determined for the state variable model given by equations (20) and (21). Using equation (30), the desired output is

$$X_{1d} = Z_d . \tag{36}$$

From equation (31) together with the definition for A and b given by equation (18), the equilibrium point and the biased input are given by

$$\begin{aligned} -VX_{2d} + VX_{4d} &= 0 \\ X_{3d} &= 0 \\ a_1X_{3d} + a_2X_{4d} &= -b_1U_d \\ a_3X_{3d} + a_4X_{4d} &= -b_2U_d . \end{aligned} \tag{37}$$

Equations (36) and (37) can be written as

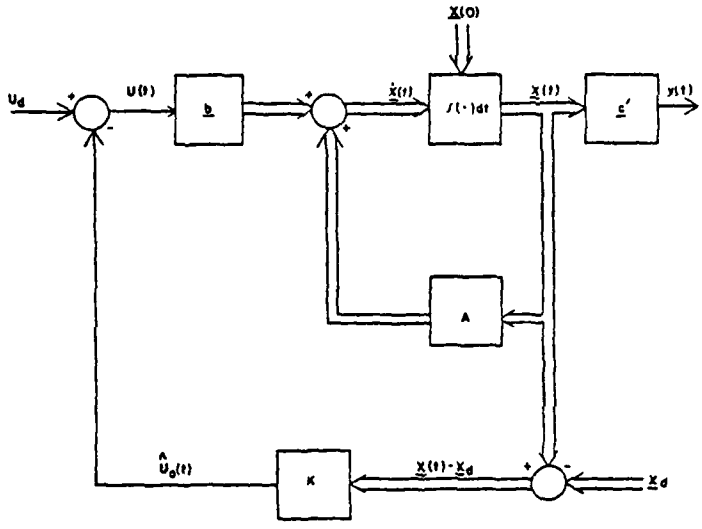


Figure 3. Closed-loop Structure of the Optimal Control Scheme

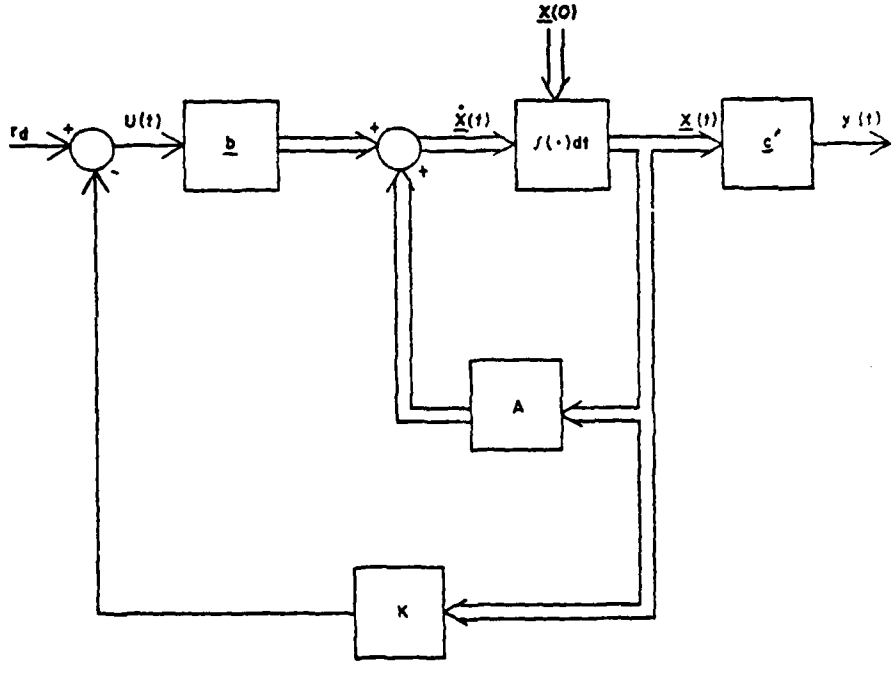


Figure 4. Alternate Closed-loop Structure of the Optimal Control Scheme

$$
\begin{aligned}
X_{1d} &= Z_d \\
X_{2d} &= X_{4d} \\
a_2 X_{4d} &= -b_1 U_d \\
a_4 X_{4d} &= -b_2 U_d \\
X_{3d} &= 0.
\end{aligned}
\tag{38}
$$

Relating equation set (38) back to its true representations shows that to maintain the underwater vehicle at a constant depth, the vehicle's depth, $X_{1d}$, must equal the desired depth, $Z_d$; the vehicle's pitch, $X_{2d}$, and angle of attack, $X_{4d}$, must be equal; and the vehicle's pitch rate, $X_{3d}$, must be zero. Solving equation set (38) for the constant biased input, $U_d$, in terms of the equilibrium states, $\underline{X}_d$, yields

$$U_d = 0. \tag{39}$$

Thus, the equilibrium states become

$$
\begin{bmatrix} X_{1d} \\ X_{2d} \\ X_{3d} \\ X_{4d} \end{bmatrix} = \begin{bmatrix} Z_d \\ 0 \\ 0 \\ 0 \end{bmatrix}. \tag{40}
$$

Substituting equations (39) and (40) into equation (35) and substituting for the gain given by equation (25b) yields

$$r_d = k_1 X_{1d} \tag{41}$$

A block diagram of the complete tracking system is shown in figure 5.

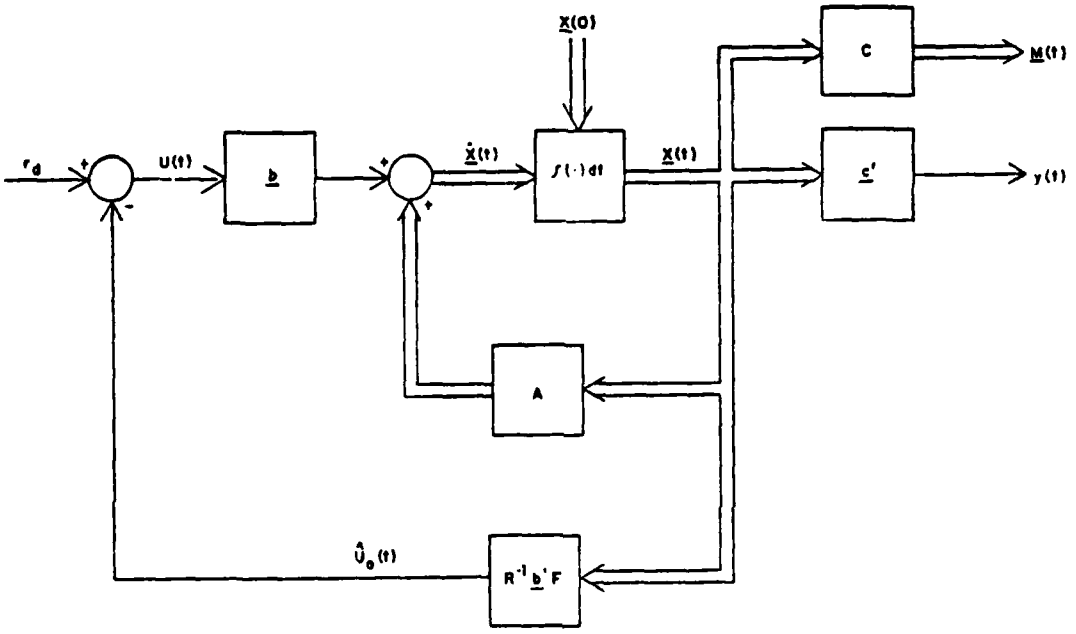


Figure 5. Block Diagram of the Tracking System

REDUCED-ORDER OBSERVER

The states $X_1(t)$, $X_2(t)$, and $X_3(t)$ are available for measurement at the output, but the state $X_4(t)$, angle of attack, is not. In order to apply optimal control theory to this system, all the states must be accessible. A reduced-order Luenberger observer (reference 10) is implemented to construct an estimate of the state $X_4(t)$.

Equations (18) and (19) are partioned in the form

$$\left[\begin{array}{c}\dot{X}_1(t)\\ \dot{X}_2(t)\\ \dot{X}_3(t)\\ \hline \dot{X}_4(t)\end{array}\right] = \left[\begin{array}{ccc:c} 0 & -V & 0 & V \\ 0 & 0 & 1 & 0 \\ 0 & 0 & a_1 & a_2 \\ \hdashline 0 & 0 & a_3 & a_4 \end{array}\right] \left[\begin{array}{c}X_1(t)\\ X_2(t)\\ X_3(t)\\ \hline X_4(t)\end{array}\right] + \left[\begin{array}{c}0\\ 0\\ b_1\\ \hline b_2\end{array}\right] U(t) \qquad (42)$$

$$\left[\begin{array}{c}m_1(t)\\ m_2(t)\\ m_3(t)\end{array}\right] = \left[\begin{array}{ccc:c} 1 & 0 & 0 & 0 \\ 0 & 1 & 0 & 0 \\ 0 & 0 & 1 & 0 \end{array}\right] \left[\begin{array}{c}X_1(t)\\ X_2(t)\\ X_3(t)\\ \hline X_4(t)\end{array}\right]. \qquad (43)$$

Make the substitutions

$$\left[\begin{array}{c}X_1(t)\\ X_2(t)\\ X_3(t)\\ \hline X_4(t)\end{array}\right] = \left[\begin{array}{c}m_1(t)\\ m_2(t)\\ m_3(t)\\ \hline Z(t)\end{array}\right] = \left[\begin{array}{c}\underline{M}(t)\\ \hline Z(t)\end{array}\right]$$

$$\left[\begin{array}{ccc:c} 0 & -V & 0 & V \\ 0 & 0 & 1 & 0 \\ 0 & 0 & a_1 & a_2 \\ \hdashline 0 & 0 & a_3 & a_4 \end{array}\right] = \left[\begin{array}{c:c} A_{11} & \underline{A}_{12} \\ \hline A_{21} & A_{22} \end{array}\right]$$

and

$$\begin{bmatrix} 0 \\ 0 \\ b_1 \\ \hline b_2 \end{bmatrix} = \left[\begin{array}{c} \underline{B}_1 \\ \hline b_2 \end{array}\right].$$

Equations (42) and (43) become

$$\left[\begin{array}{c} \dot{\underline{M}}(t) \\ \hline \dot{Z}(t) \end{array}\right] = \left[\begin{array}{c|c} A_{11} & \underline{A}_{12} \\ \hline A_{21} & A_{22} \end{array}\right] \left[\begin{array}{c} \underline{M}(t) \\ \hline Z(t) \end{array}\right] + \left[\begin{array}{c} \underline{B}_1 \\ \hline b_2 \end{array}\right] U(t) \quad . \tag{44}$$

Equation (44) is written as a reduced plant and an output equation of the form

$$\dot{Z}(t) = A_{22}Z(t)+A_{21}\underline{M}(t)+b_2U(t) \tag{45a}$$

$$\dot{\underline{M}}(t) - A_{11}\underline{M}(t)-\underline{B}_1U(t) = \underline{A}_{12}Z(t) \, . \tag{45b}$$

The vector $\underline{M}(t)$ is available for measurement; if $\underline{M}(t)$ is differentiated, then $\dot{\underline{M}}(t)$ is also available. Since $U(t)$ is also measurable, equation (45b) provides the measurement $\underline{A}_{12}\underline{Z}(t)$ for the system described by equation (45a), which has state $Z(t)$ and input $A_{21}\underline{M}(t) + b_2U(t)$. Equation (45) is written as

$$\dot{Z}(t) = A_{22}Z(t) + \overline{B}\,\overline{U}(t) \tag{46a}$$

$$\overline{\underline{M}}(t) = \overline{\underline{C}}\, Z(t) \tag{46b}$$

where

$$\bar{B} = [A_{21} \quad b_2], \quad \underline{\bar{U}}(t) = \begin{bmatrix} \underline{M}(t) \\ \hline U(t) \end{bmatrix}, \quad \underline{\bar{M}}(t) = \dot{\underline{M}}(t) - A_{11}\underline{M}(t) - \underline{B}_1 U(t)$$

and

$$\bar{\underline{C}} = \underline{A}_{12}.$$

Let the input, $\bar{B}\,\underline{\bar{U}}(t)$, and the output, $\underline{\bar{M}}(t)$, be used to drive another system, $\hat{Z}(t)$, such that the output of the new system approximates the state of the original system, $Z(t)$. The new system is defined as

$$\dot{\hat{Z}}(t) = F\,\hat{Z}(t) + L\,\bar{\underline{C}}Z(t) + T\,\bar{B}\,\underline{\bar{U}}(t) \tag{47}$$

where T is a transformation defined (from reference 11) by

$$T\,A_{22} - FT = L\bar{\underline{C}}.$$

The error between the real state and the estimated state is given by

$$\dot{\tilde{Z}}(t) = T\,\dot{Z}(t) - \dot{\hat{Z}}(t) = F[T\,Z(t) - \hat{Z}(t)]. \tag{48}$$

The solution to the error state equation becomes

$$\tilde{Z}(t) = {}_{\varepsilon}FT\,[T\,Z(0) - \hat{Z}(0)]. \tag{49}$$

If the new system is of the same dynamic order as the real system, then the transformation T can become an identity matrix and the new system becomes an identity observer of the form

$$\dot{\hat{Z}}(t) = [A_{22} - L\,\bar{\underline{C}}]\,\hat{Z}(t) + L\,\bar{\underline{C}}Z(t) + \bar{B}\,\underline{\bar{U}}(t). \tag{50}$$

Substituting

$$F = A_{22} - L\,\underline{\bar{C}} \quad \text{and} \quad \tilde{Z} = Z(t) - \hat{Z}(t)$$

into the error state equation results in

$$\dot{\tilde{Z}}(t) = [A_{22} - L\,\underline{\bar{C}}]\,\tilde{Z}(t). \tag{51}$$

The eigenvalue of equation (51) may be selected by the proper selection of the matrix L, which is given by

$$L = [l_1 \quad l_2 \quad l_3],$$

where $l_1$, $l_2$, and $l_3$ are scalars. By being able to control the selection of the eigenvalue of $[A_{22} - L\,\underline{\bar{C}}]$, the behavior of the error, $\tilde{Z}(t)$, can be controlled. The solution to equation (51) is given by

$$\tilde{Z}(t) = \varepsilon^{\sigma t}\,\tilde{Z}(0), \tag{52}$$

where $\sigma$ denotes the eigenvalue of $[A_{22} - L\,C]$. Equation (52) shows that as long as the eigenvalue is negative, the error, $\tilde{Z}(t)$, will approach zero regardless of the initial error, $\tilde{Z}(0)$. The eigenvalue of the state estimator is arbitrary, but it must be negative so that the error will converge to zero.

Substituting for $\bar{B}$, $\underline{\bar{U}}(t)$, and $\bar{C}$ in equation (50) and using equation (45b), an identity observer of the form

$$\begin{aligned}\dot{\hat{Z}}(t) = {} & [A_{22} - L\,\underline{A}_{12}]\,\hat{Z}(t) + L\,\dot{\underline{M}}(t) + [A_{21} - L\,A_{11}]\underline{M}(t) \\ & + [b_2 - LB_1]\,U(t)\end{aligned} \tag{53}$$

is obtained.

The observer contains a differentiation of $\underline{M}(t)$. To eleiminate the differentiation, let

$$\dot{\hat{Z}}(t) = \dot{W}(t) + L\,\dot{\underline{M}}(t)$$

and

$$\hat{Z}(t) = W(t) + L\,\underline{M}(t). \tag{54}$$

This yields a new estimator, eliminating the differentiation of $\underline{M}(t)$ of the form

$$\dot{W}(t) = [A_{22} - L\,\underline{A_{12}}]W(t) + \{[A_{21} - L\,A_{11}] + [A_{22} - L\,\underline{A_{12}}]L\}\,\underline{M}(t) + [b_2 - L\,\underline{B_1}]\,U(t). \tag{55}$$

Figure 6 shows the configuration of the reduced state estimator.

The eigenvalue of the observer is arbitrary. Once the system is modeled on the computer, the eigenvalue can be adjusted so that a good estimate of the state will be obtained. Let the eigenvalue of the estimator be $-\sigma$ ($\sigma>0$). Then, from equation (51), the characteristic equation is

$$\lambda - a_4 + l_1 V + l_3 a_2 = 0\,. \tag{56}$$

Since the estimator has an eigenvalue at $-\sigma$, the characteristic equation is

$$\lambda + \sigma = 0. \tag{57}$$

Matching the coefficients of equations (56) and (57) yields

$$l_1 V + l_3 a_2 = \sigma + a_4\,. \tag{58}$$

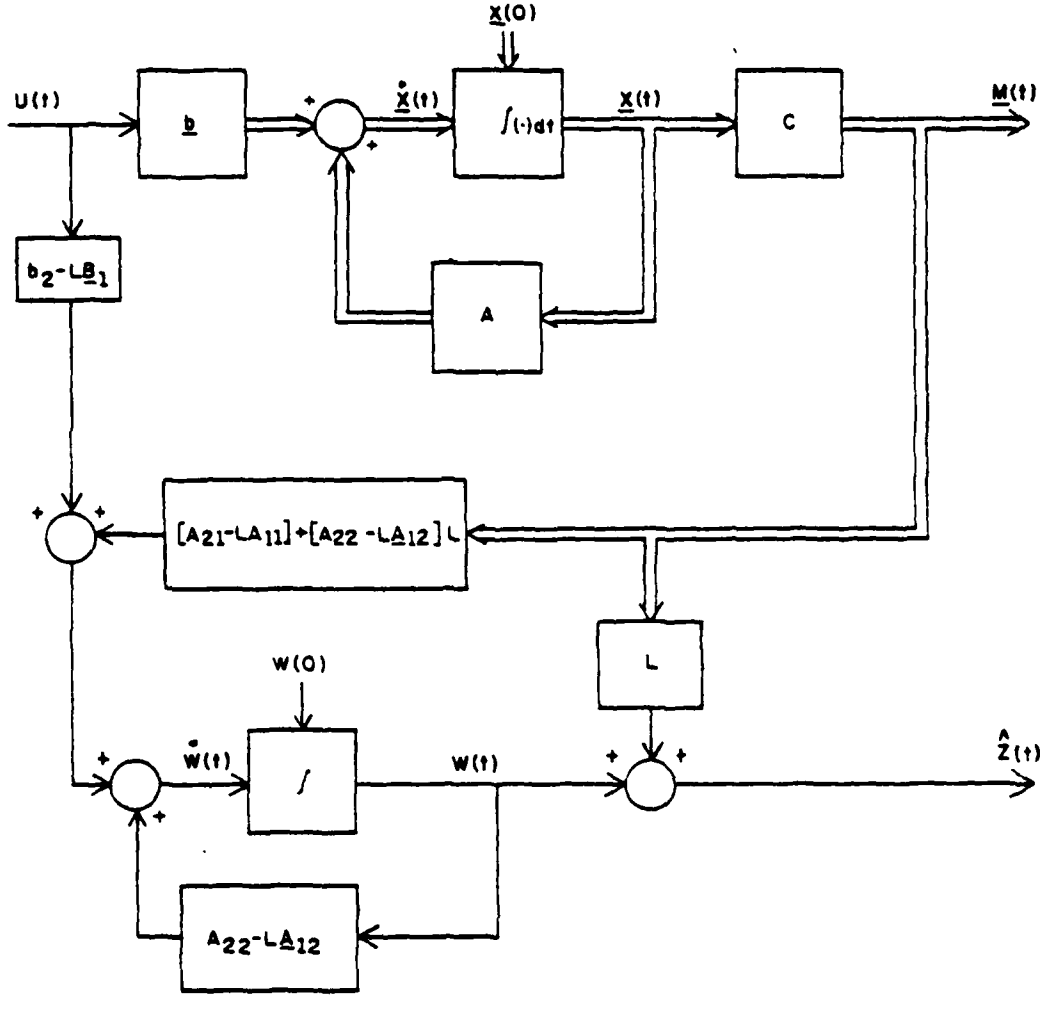


Figure 6. Reduced-order Luenberger Observer

The element $l_2$ does not enter into the selection of the eigenvalue. Therefore, it is arbitrary and can be set to zero. If $l_1$ is selected to be zero, then, from equation (58), the element $l_3$ becomes

$$l_3 = \frac{\sigma + a_4}{a_2} \quad .$$

Equation (55) is now given by

$$\dot{W}_1(t) = -\sigma W_1(t) + [a_3 - \frac{(\sigma+a_4)(\sigma+a_1)}{a_2}] m_3(t) + [b_2 - \frac{b_1(\sigma+a_4)}{a_2}]U(t). \tag{59}$$

To obtain an estimate of angle of attack, $W_1(t)$ is solved for in equation (59) and substituted into equation (54).

Selecting $l_3$ to be zero and solving for the element $l_1$ in equation (58) results in a new estimator of the form

$$\dot{W}_2(t) = -\sigma W_2(t) - \frac{\sigma(\sigma+a_4)}{V} m_1(t) + (\sigma+a_4)m_2(t) + a_3 m_3(t) + b_2 U(t). \tag{60}$$

Using equations (54) and (60), an estimate of the angle of attack, $X_4(t)$, is obtained. Even though two different equations are used as an estimator (other estimators may be formulated containing both $l_1$ and $l_3$ elements), the error state equation (equation (51)) and the transfer functions of the estimators are identical. Because the estimator given by equation (60) uses three measurements, it is more susceptible to modeling errors, since any error in the signal $m_3(t)$ is integrated into the $m_2(t)$ signal

and the net effect is a larger error. Therefore, equation (59) is used in lieu of equation (6) as the estimator.

The term $\hat{Z}(t)$ in equation (54) provides an estimate of the angle of attack, $X_4(t)$. If the observer is selected properly, the transfer functions $\frac{X_4(t)}{U(t)}$ and $\frac{\hat{Z}(t)}{U(t)}$ are the same. Appendix D demonstrates that the two transfer functions are equal. A block diagram of the complete system is shown in figure 7.

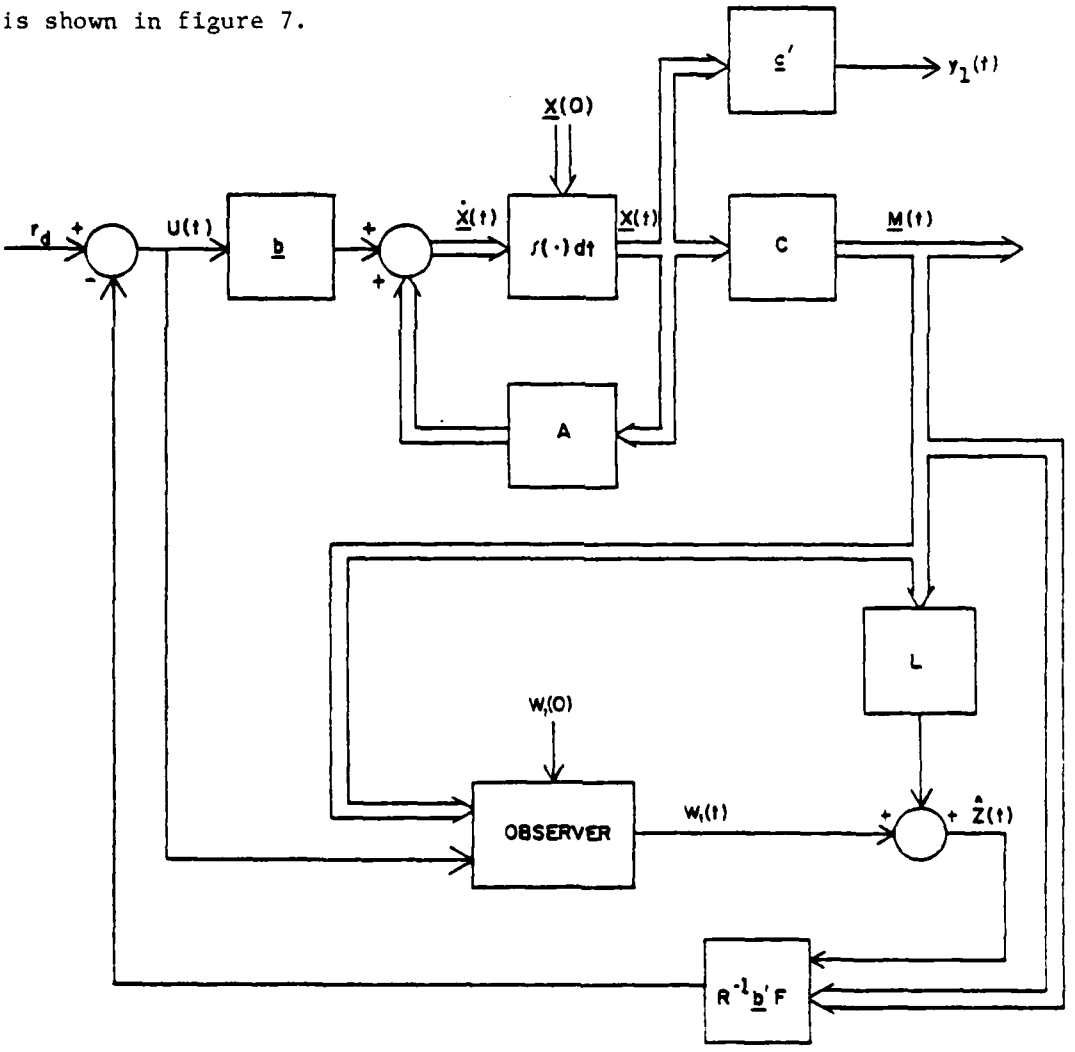


Figure 7. Block Diagram of the Complete Closed-loop Control Scheme

## MODIFIED SOLUTION TO THE TRACKING PROBLEM

The optimal control law was formulated for an underwater vehicle that was neutrally buoyant with coincident centers of gravity and buoyancy. A modified optimal control law is developed in this section for the general state variable model described by equation (16), and is repeated here as

$$\dot{\underline{X}}(t) = \overline{A}\underline{X}(t) + \overline{\underline{b}}\, U(t) + \underline{d} \tag{61}$$

The constant bias, $\underline{d}$, is included in the state variable model as a constant step. Equations (13) and (14) reveal that the angle of attack, state, and the input control, U(t), have non-zero steady state values due to the constant bias, and equation (12) shows that the pitch and angle of attack states must be equal. Inclusion of the constant bias into the solution of the tracking problem is accomplished by the alteration of the desired equilibrium states, $\underline{X}_d$, and the desired constant biased input, $U_d$, in equation (31). The relationship between the equilibrium states and the constant biased input becomes

$$\overline{A}\underline{X}_d + \overline{\underline{b}}\, U_d = -\underline{d} \ . \tag{62}$$

Using equations (30) and (62), the equilibrium states and the biased input are given by

$$\begin{aligned} X_{1d} &= Z_d \\ -VX_{2d} + VX_{4d} &= 0 \\ X_{3d} &= 0 \end{aligned}$$

$$\bar{a}_1 X_{3d} + \bar{a}_2 X_{4d} = -\bar{b}_1 U_d - \bar{d}_1$$
$$\bar{a}_3 X_{3d} + \bar{a}_4 X_{4d} = -\bar{b}_2 U_d - \bar{d}_2 .$$

The equilibrium states and the biased input can be written in terms of the constant coefficients as

$$\begin{bmatrix} X_{1d} \\ X_{2d} \\ X_{3d} \\ X_{4d} \end{bmatrix} = \begin{bmatrix} Z_d \\ \dfrac{\bar{b}_1 \bar{d}_2 - \bar{b}_2 \bar{d}_1}{\bar{b}_2 \bar{a}_2 - \bar{b}_1 \bar{a}_4} \\ 0 \\ X_{2d} \end{bmatrix} \tag{63}$$

and

$$U_d = \frac{\bar{d}_1 \bar{a}_4 - \bar{d}_1 \bar{a}_2}{\bar{b}_2 \bar{a}_2 - \bar{b}_1 \bar{a}_4} . \tag{64}$$

Substituting equations (63) and (64) into equation (35) results in a desired reference signal of the form

$$r_d = \frac{\bar{d}_1 \bar{a}_4 - \bar{d}_2 \bar{a}_2}{\bar{b}_2 \bar{a}_2 - \bar{b}_1 \bar{a}_4} + K_1 X_{1d} + K_2 \frac{\bar{b}_1 \bar{d}_2 - \bar{b}_2 \bar{d}_1}{\bar{b}_2 \bar{a}_2 - \bar{b}_1 \bar{a}_4} + K_4 \frac{\bar{b}_1 \bar{d}_2 - \bar{b}_2 \bar{d}_1}{\bar{b}_2 \bar{a}_2 - \bar{b}_1 \bar{a}_4} . \tag{65}$$

A block diagram of the modified tracking system is shown in figure 8.

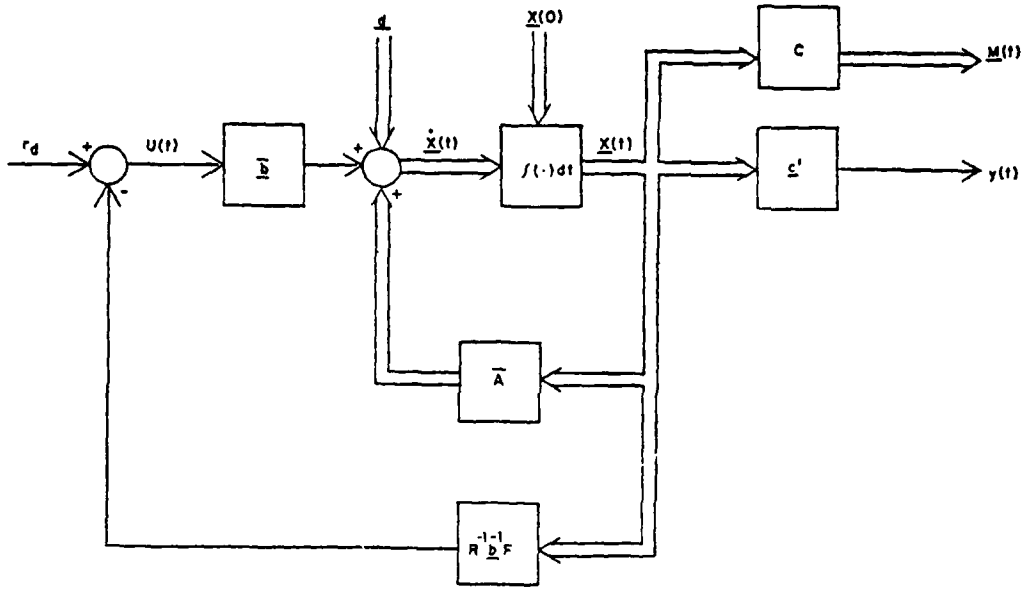


Figure 8. Block Diagram of the Modified Tracking System

From equation (63), it is seen that to maintain an underwater vehicle at a constant depth, the desired pitch and angle of attack states are no longer zero. In order for the states to have non-zero values, the desired input, $U_d$, must have a non-zero value as shown by equation (64).

## MODIFICATIONS TO THE REDUCED-ORDER OBSERVER

The reduced-order observer must be altered to include the addition of the constant bias in the state variable model given by equation (61). Using the same techniques in developing the reduced-order observer in Section II, the modified observer will be constructed in this section.

Partitioning the state variable model in the form

$$\left[\begin{array}{c}\dot{X}_1(t)\\ \dot{X}_2(t)\\ \dot{X}_3(t)\\ \hline \dot{X}_4(t)\end{array}\right] = \left[\begin{array}{ccc:c}0 & -V & 0 & V\\ 0 & 0 & 1 & 0\\ 0 & 0 & \bar{a}_1 & \bar{a}_2\\ \hline 0 & 0 & \bar{a}_3 & \bar{a}_4\end{array}\right] \left[\begin{array}{c}X_1(t)\\ X_2(t)\\ X_3(t)\\ \hline X_4(t)\end{array}\right] + \left[\begin{array}{c}0\\ 0\\ \bar{b}_1\\ \hline \bar{b}_2\end{array}\right] U(t) + \left[\begin{array}{c}0\\ 0\\ \bar{b}_3\\ \hline \bar{b}_4\end{array}\right] \tag{66a}$$

and

$$\left[\begin{array}{c}M_1(t)\\ M_2(t)\\ M_3(t)\end{array}\right] = \left[\begin{array}{ccc:c}1 & 0 & 0 & 0\\ 0 & 1 & 0 & 0\\ 0 & 0 & 1 & 0\end{array}\right] \left[\begin{array}{c}X_1(t)\\ X_2(t)\\ X_3(t)\\ X_4(t)\end{array}\right] \tag{66b}$$

and letting

$$\bar{A}_{11} = \begin{bmatrix}0 & -V & 0\\ 0 & 0 & 1\\ 0 & 0 & \bar{a}_1\end{bmatrix}, \quad \underline{\bar{A}}_{12} = \begin{bmatrix}V\\ 0\\ \bar{a}_2\end{bmatrix}, \quad \bar{A}_{21} = [0 \quad 0 \quad \bar{a}_3], \quad \bar{A}_{22} = \bar{a}_4,$$

$$\underline{B}_1 = \begin{bmatrix}0\\ 0\\ \bar{b}_1\end{bmatrix} \quad \text{and} \quad \underline{B}_2 = \begin{bmatrix}0\\ 0\\ \bar{b}_3\end{bmatrix}$$

results in a reduced plant and output equation of the form

$$\dot{\bar{Z}}(t) = \bar{A}_{22}\,\bar{Z}(t) + \bar{D}\,\underline{\bar{U}}(t) \tag{67}$$

and

$$\tilde{\underline{M}}(t) = \tilde{\underline{C}}\ \overline{Z}(t) \tag{68}$$

where

$$\overline{D} = [\overline{A}_{21} \quad \overline{b}_2 \quad \overline{b}_4],\ \tilde{\underline{U}}(t) = \begin{bmatrix} \underline{M}(t) \\ U(t) \\ 1 \end{bmatrix},$$

$$\tilde{\underline{M}}(t) = \dot{\underline{M}}(t) - \overline{A}_{11}\ \underline{M}(t) - \underline{B}_1\ U(t) - \underline{B}_2 \quad \text{and} \quad \tilde{\underline{C}} = \overline{A}_{12}\ .$$

Substituting equations (67) and (68) into equation (50) of an identity observer results in a modified reduced-order observer of the form

$$\dot{\hat{\overline{Z}}}(t) = [\overline{A}_{22} - \overline{L}\ \tilde{\underline{C}}]\ \hat{\overline{Z}}(t) + \overline{L}\ \tilde{\underline{C}}\ \overline{Z}(t) + \overline{D}\ \tilde{\underline{U}}(t). \tag{69}$$

Substituting for $\overline{D}$, $\tilde{\underline{U}}(t)$, $\tilde{\underline{M}}(t)$ and $\tilde{\underline{C}}$ in equation (69) yields

$$\dot{\hat{\overline{Z}}}(t) = [\overline{A}_{22} - \overline{L}\ \tilde{\underline{C}}]\ \hat{\overline{Z}}(t) + \overline{L}[\dot{\underline{M}}(t) - \overline{A}_{11}\ \underline{M}(t) - \underline{B}_1\ U(t) - \underline{B}_2]$$

$$+ \overline{A}_{21}\ \underline{M}(t) + \overline{b}_2\ U(t) + \overline{b}_4\ .$$

To eliminate the differentiation let

$$\dot{\hat{\overline{Z}}}(t) = \dot{\overline{W}}(t) + \overline{L}\ \dot{\underline{M}}(t)$$

and

$$\hat{\overline{Z}}(t) = \overline{W}(t) + \overline{L}\ \underline{M}(t)$$

which results in a new estimator of the form

$$\dot{\bar{W}}(t) = [A_{22} - \bar{L}\,\underline{\bar{C}}]\,W(t) + \{[\bar{A}_{22} - \bar{L}\,\underline{\bar{A}}_{12}]\bar{L} + [\bar{A}_{21} - \bar{L}\,\bar{A}_{11}]\}\,\underline{M}(t)$$

$$+ [\bar{b}_2 - \bar{L}\,\underline{B}_1]\,U(t) + \bar{b}_4 - \bar{L}\,\underline{B}_2\,. \qquad (70)$$

The matrix of the observer is found in the same manner as in the previous section and is given by

$$\bar{L} = [0 \quad 0 \quad \frac{\bar{\sigma}+\bar{a}_4}{\bar{a}_2}\,].$$

Substituting for $\bar{L}$ in equation (70) results in a modified observer of the form

$$\dot{\bar{W}}(t) = -\bar{\sigma}\,\bar{W}(t) + [\bar{a}_3 - \frac{\bar{a}_1(\bar{\sigma}+\bar{a}_4)}{\bar{a}_2} - \frac{\bar{\sigma}(\bar{\sigma}+\bar{a}_4)}{\bar{a}_2}\,]\,M_3(t)$$

$$+ [\bar{b}_2 - \frac{\bar{b}_1(\bar{\sigma}+\bar{a}_4)}{\bar{a}_2}]\;U(t) + \bar{b}_4 - \frac{\bar{b}_3(\bar{\sigma}+\bar{a}_4)}{\bar{a}_2}\,. \qquad (71)$$

# SECTION IV

## RESULTS OF LABORATORY RUNS

The closed-loop control scheme for the underwater vehicle shown in figure 7 was simulated on a digital computer using the hydrodynamic coefficients of a typical torpedo traveling at a constant speed. The state transition matrix developed in appendix C was used to solve the state equations; and the steady state solution to the matrix Riccati equation was found using a standard numerical integration technique. Included in the control scheme were limitations of 30 degrees for vehicle pitch and rudder deflection. Plots were made of the torpedo's depth, pitch, pitch rate, angle of attack, and rudder angle (input control). Since a Luenberger observer was used to estimate the angle of attack, a plot of the estimator error was also included. The weighting terms in the performance index were varied to achieve the best performance for the torpedo; i.e., minimum time to reach the desired depth. Table 1 contains a summary of all the torpedo trajectories.

In the first set of plots, the torpedo was initially at 50 meters, diving to a desired depth of 100 meters at a constant speed of 25 meters/sec. Figure 9a shows that the torpedo arrives at the desired depth at approximately 5 seconds; vehicle pitch, pitch rate, angle of attack, and rudder angle approach the desired values as shown in figures 9b, 9c, 9d, and 9f. The plot of the observer error, figure

9e, shows that there is a small initial error during the first 5 seconds of the run until the angle of attack approaches its steady state value (figure 9d). At this time, the observer error goes to zero. In this set of plots, the initial conditions on the observer and the angle of attack are identical. In the next set of plots, figure 10, there is a 10-degree difference between the initial conditions. There is no significant change between the plots of figure 9 and figure 10, except in the plot of the angle of attack error, figure 10e. Because of the large vertical scale and small observer error, the observer error appears to be zero. However, there is an initial observer error of 10 degrees which approaches zero rapidly because of the large observer pole. Changing the observer eigenvalue to a smaller value and rerunning the trajectory increases the time for the observer error to approach zero (see figure 11). This time increase also has a small effect on the angle of attack, which is seen by comparing figures 10d and 11d. The angle of attack takes on different initial values until the torpedo reaches its desired depth. There are also small changes in the other states, but these changes cannot be detected in the plots. The trajectory of figure 9 was rerun using the actual angle of attack in place of the estimated value in determining the optimal control law. Figure 12 shows that the change in the performance of the controller is insignificant.

In all of the trajectories that were simulated (figures 9 through 12), the pitch angle and the rudder deflection angle reached their saturation points. By changing the weighting terms in the performance index, the amount of deflection can be altered. The weighting term which regulates deviations in vehicle depth was reduced, and a plot of this trajectory is shown in figure 13. From this plot, it is seen that the pitch angle and the rudder deflection angle do not reach the saturation levels, but comparing figures 9a and 13a shows that the time for the torpedo to reach its desired depth has been increased. Increasing the weighting on the vehicle depth error has a reverse effect and can cause the torpedo to oscillate about the desired trajectory, as can be seen in figure 14, which shows that the states overshoot their desired values and oscillate about them while approaching the desired values.

The speed of the vehicle has an effect on the performance of the controller. Even though the speed could have been normalized out of the state variable model (reference 2), an optimal control law can be found for various vehicle speeds. The trajectory of figure 9 was run with a 50 percent reduction in torpedo speed. The plots for this case are shown in figure 15. Comparing figures 9 and 15, it is seen that the plots are similar, but the torpedo takes longer to reach the desired depth in figure 15a, as would be expected. Increasing the weighting on the depth error, figure 16, provides little improvement on the performance of the torpedo.

The non-neutrally buoyant vehicle with different centers of gravity and buoyancy was also simulated. The trajectory of figure 15 was used and the plots are shown in figure 17. In this set of plots, the desired trajectories of the pitch and angle of attack take on non-zero values in order to keep the torpedo from sinking. Once the torpedo reaches the des ed depth, the pitch and angle of attack approach the desired trajectories. The steady state values for the pitch and angle of attack are small (see table 1), but the amount of rudder deflection necessary to maintain these values is large, as can be seen from figure 17f.

When an underwater vehicle operates near the surface in a high sea state condition, ocean currents may cause the vehicle to deviate from its desired trajectory. These seaway disturbances were incorporated into the closed-loop tracking scheme as a known constant bias caused by the vertical velocity of the water particles. Figure 18 demonstrates the performance of the controller for a torpedo operating under these conditions. The torpedo is at an initial depth of 50 meters climbing to a desired depth of 2 meters. It is assumed that the seaway disturbance had a constant effect on the torpedo throughout the trajectory with a vertical velocity of 1 meter/sec. From the plots, it is seen that the states approach their desired values. Since the pitch and angle of attack no longer have zero steady state values, the rudder deflection angle (input control) also takes on a non-zero steady state value.

Comparing figures 17 and 18, it is interesting to note that the desired inputs are the same, but there is a significant difference between the steady state values of the pitch and angle of attack. By examining equation (64) and substituting for the terms $d_1$ and $d_2$ from equations (11e) and (11f) and the terms $a_2$ and $a_4$ from equations (8f) and (9h), the desired input becomes

$$U_d = \frac{\bar{b}_3\bar{a}_4 - \frac{(mX_gJ_yZ_wZ_\alpha + m_tmX_gM_wM_\alpha)V_w}{V\beta^2} - \bar{b}_4\bar{a}_2 + \frac{(mX_gJ_yZ_wZ_\alpha + m_tmX_gM_wM_\alpha)V_w}{V\beta^2}}{\bar{b}_2\bar{a}_2 - \bar{b}_1\bar{a}_4},$$

which reduces to

$$U_d = \frac{\bar{b}_3\bar{a}_4 - \bar{b}_4\bar{a}_2}{\bar{b}_2\bar{a}_2 - \bar{b}_1\bar{a}_4}$$

and is independent of the vertical velocity of the water.

The simulations have shown that the linear mean-square optimal control law is a favorable approach in the control of an underwater vehicle. By changing the weighting terms in the performance index, desirable trajectories of various underwater vehicles can be achieved over a wide range of speeds. For the example shown it was found that the weighting terms used in figure 9 yielded a satisfactory

performance of the controller, and that an observer eigenvalue that was of slightly greater magnitude than the eigenvalues of the closed-loop system achieved the best results. It was also found that there was no need to change the performance index weighting terms when there was a 50 percent reduction in speed.

Table 1. Summary of Torpedo Trajectories

| Figure | P.I. Weighting | | Torpedo Velocity (m/sec) | Observer Eigenvalues | Observer Initial Conditions (deg) | Closed-loop Control Scheme Eigenvalues | | | |
|---|---|---|---|---|---|---|---|---|---|
| | Q | R | | | | $P_1$ | $P_2$ | $P_3$ | $P_4$ |
| 9 | .002 | 15 | 25 | -30 | 0 | -6.98 | -28.95 | -.6+j.6 | -.6-j.6 |
| 10 | .002 | 15 | 25 | -30 | 10 | -6.98 | -28.95 | -.6+j.6 | -.6-j.6 |
| 11 | .002 | 15 | 25 | - 1 | 10 | -6.98 | -28.95 | -.6+j.6 | -.6+j.6 |
| 12* | .002 | 15 | 25 | -30 | 0 | -6.98 | -28.95 | -.6+j.6 | -.6+j.6 |
| 13 | .0001 | 15 | 25 | -30 | 0 | -6.98 | -28.95 | -.287+j.289 | -.287-j.289 |
| 14 | 1.0 | 15 | 25 | -30 | 0 | -7.23 | -28.95 | -2.7+j3 | -2.7-j3 |
| 15 | .002 | 15 | 12.5 | -30 | 0 | -3.49 | -14.48 | -.3+j.3 | -.3-j.3 |
| 16 | .01 | 15 | 12.5 | -30 | 0 | -3.49 | -16.48 | -.45+j.45 | -.45-j.45 |
| 17 | .002 | 15 | 12.5 | -30 | 0 | -3.37 | -14.54 | -.31+j.31 | -.31-j.31 |
| 18 | .002 | 15 | 12.5 | -30 | 0 | -3.37 | -14.56 | -.31+j.31 | -.31-j.31 |

* The state $X_4(t)$ is used in determining the optimal control law

| Figure | Initial Conditions on States | | | | Desired Values for States | | | | Desired Input |
|---|---|---|---|---|---|---|---|---|---|
| | $X_1(0)$ (m) | $X_2(0)$ (deg) | $X_3(0)$ (deg/sec) | $X_4(0)$ (deg) | $X_{1d}$ (m) | $X_{2d}$ (deg) | $X_{3d}$ (deg/sec) | $X_{4d}$ (deg) | Ud (deg) |
| 9 | 50 | 0 | 0 | 0 | 100 | 0 | 0 | 0 | 0 |
| 10 | 50 | 0 | 0 | 0 | 100 | 0 | 0 | 0 | 0 |
| 11 | 50 | 0 | 0 | 0 | 100 | 0 | 0 | 0 | 0 |
| 12* | 50 | 0 | 0 | 0 | 100 | 0 | 0 | 0 | 0 |
| 13 | 50 | 0 | 0 | 0 | 100 | 0 | 0 | 0 | 0 |
| 14 | 50 | 0 | 0 | 0 | 100 | 0 | 0 | 0 | 0 |
| 15 | 50 | 0 | 0 | 0 | 100 | 0 | 0 | 0 | 0 |
| 16 | 50 | 0 | 0 | 0 | 100 | 0 | 0 | 0 | 0 |
| 17 | 50 | .17 | 0 | .17 | 100 | .17 | 0 | .17 | 3.6 |
| 18 | 50 | 4.7 | 0 | 4.7 | 2 | 4.7 | 0 | 4.7 | 3.6 |

* The state $X_4(t)$ is used in determining the optimal control law

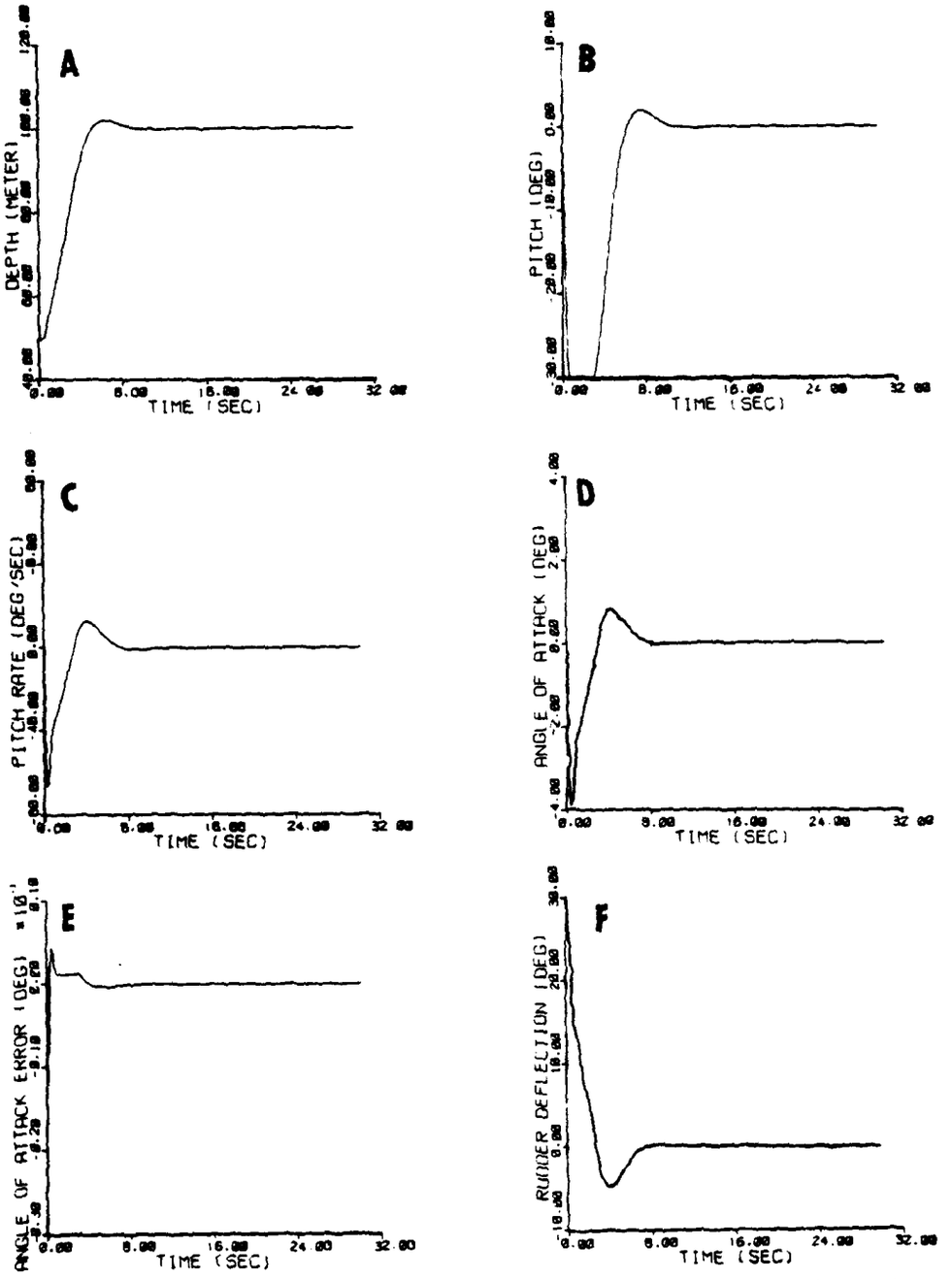


Figure 9. Optimal Trajectories for a Neutrally Buoyant Torpedo in a 50-meter Dive at a Constant Speed of 25 Meters/sec

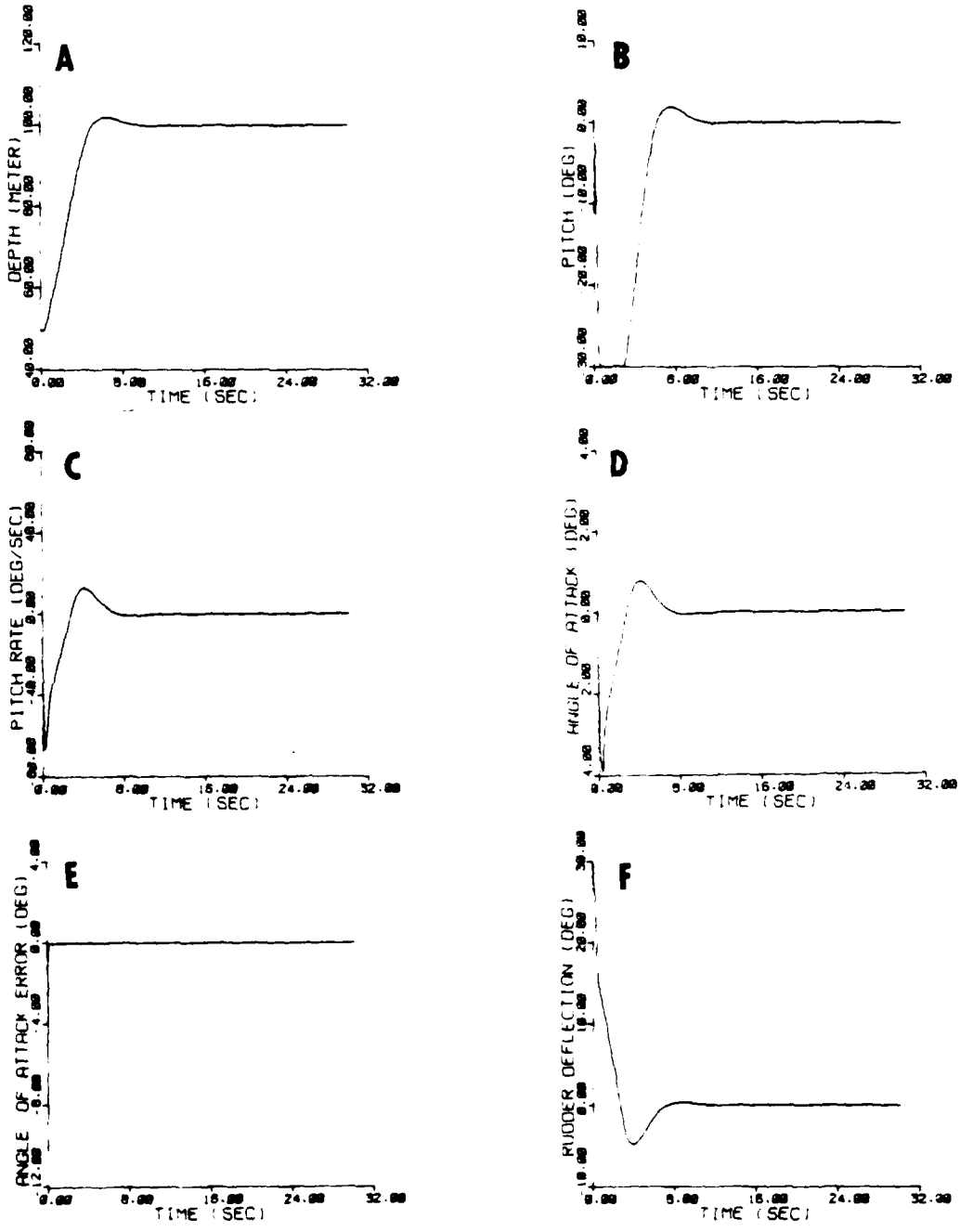


Figure 10. Optimal Trajectories with a Change in Observer Initial Conditions

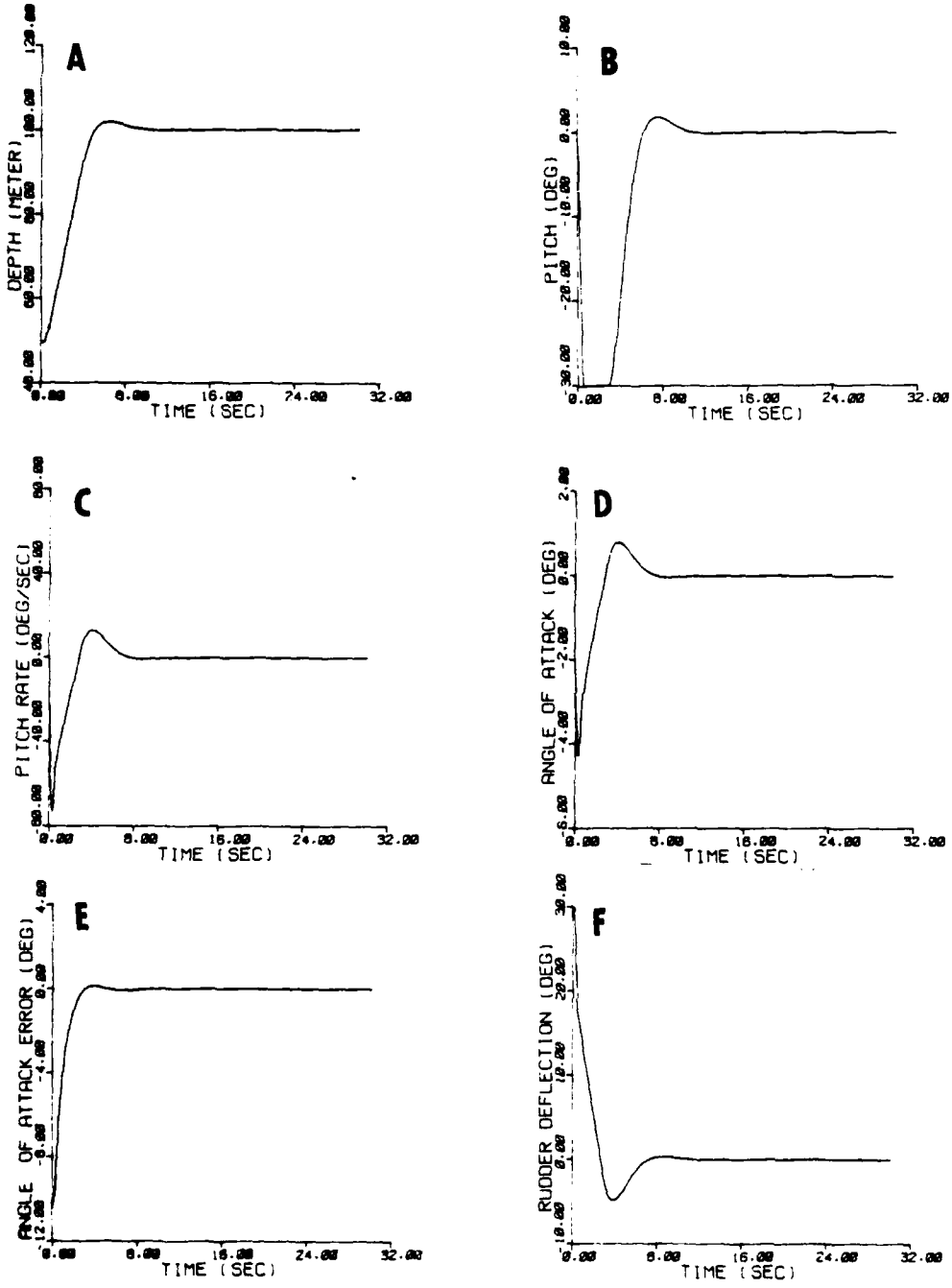


Figure 11. Optimal Trajectories with Changes in Observer Initial Conditions and Eigenvalue

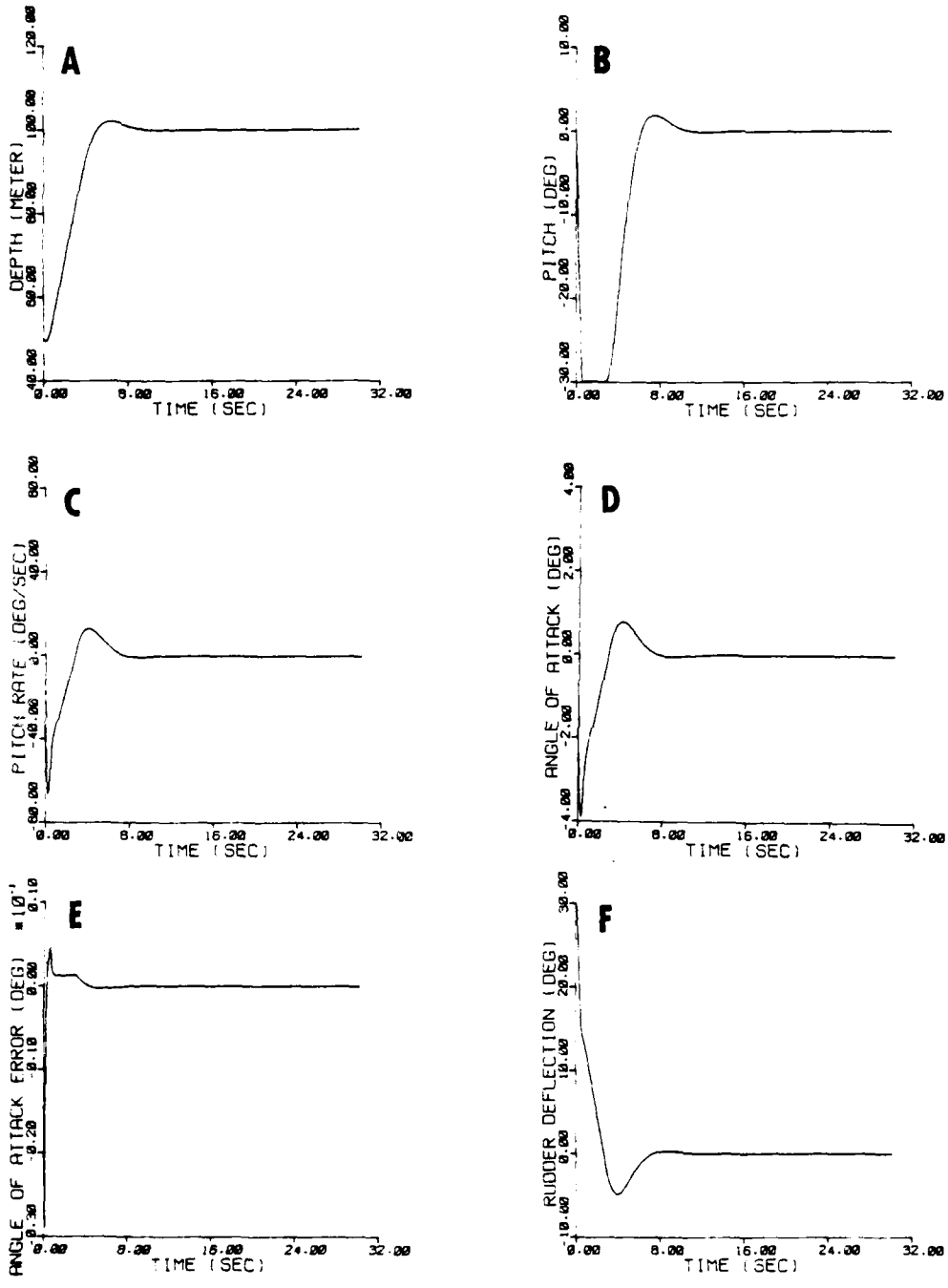


Figure 12. Optimal Trajectories with $X_4(t)$ Used in Control Law Computation

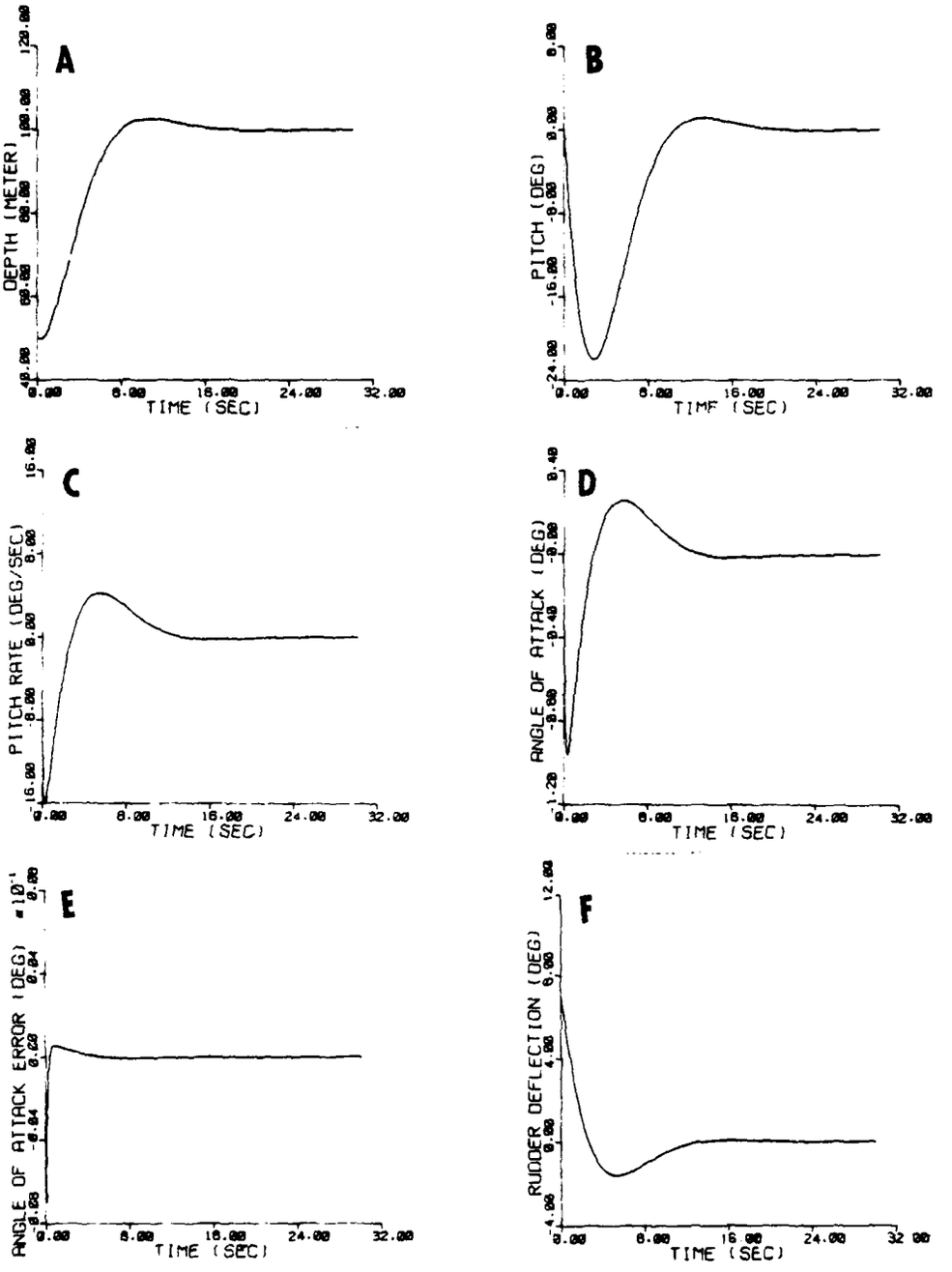


Figure 13. Optimal Trajectories With a Smaller Penalty for Depth Errors

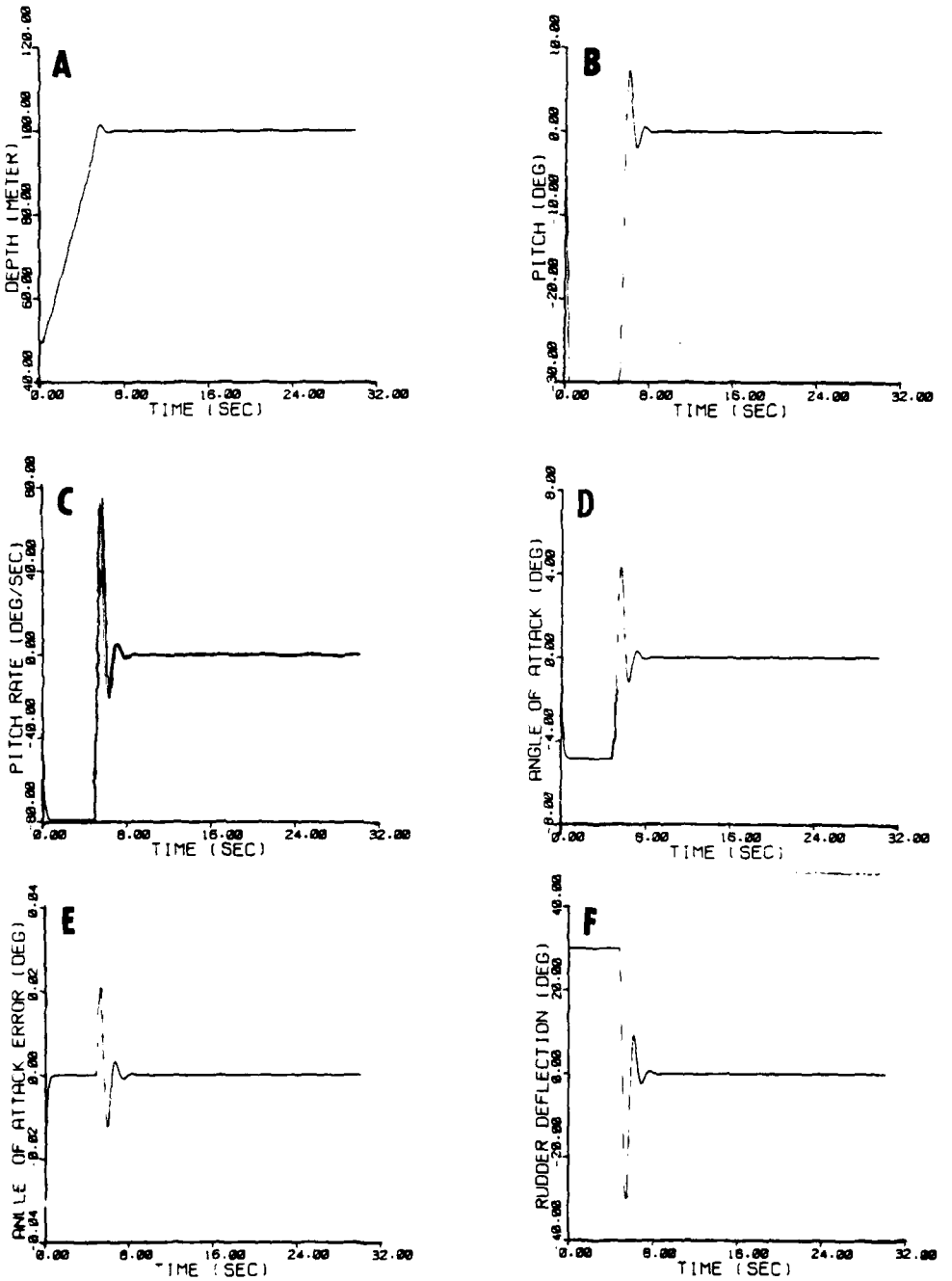


Figure 14. Optimal Trajectories With a Greater Penalty for Depth Errors

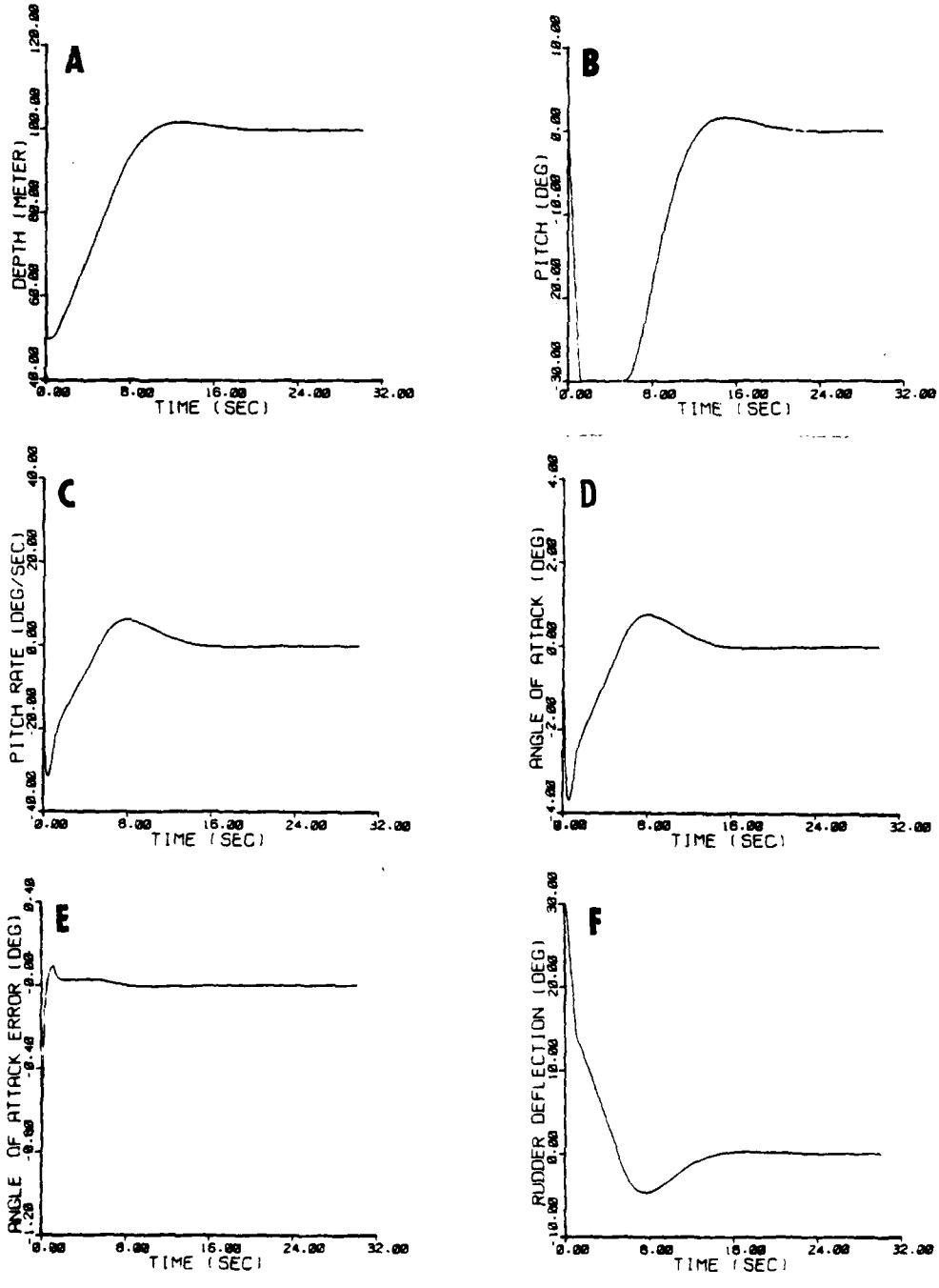


Figure 15. Optimal Trajectories for a Neutrally Buoyant Torpedo in a 50-meter Dive at a Constant Speed of 12.5 Meters/sec

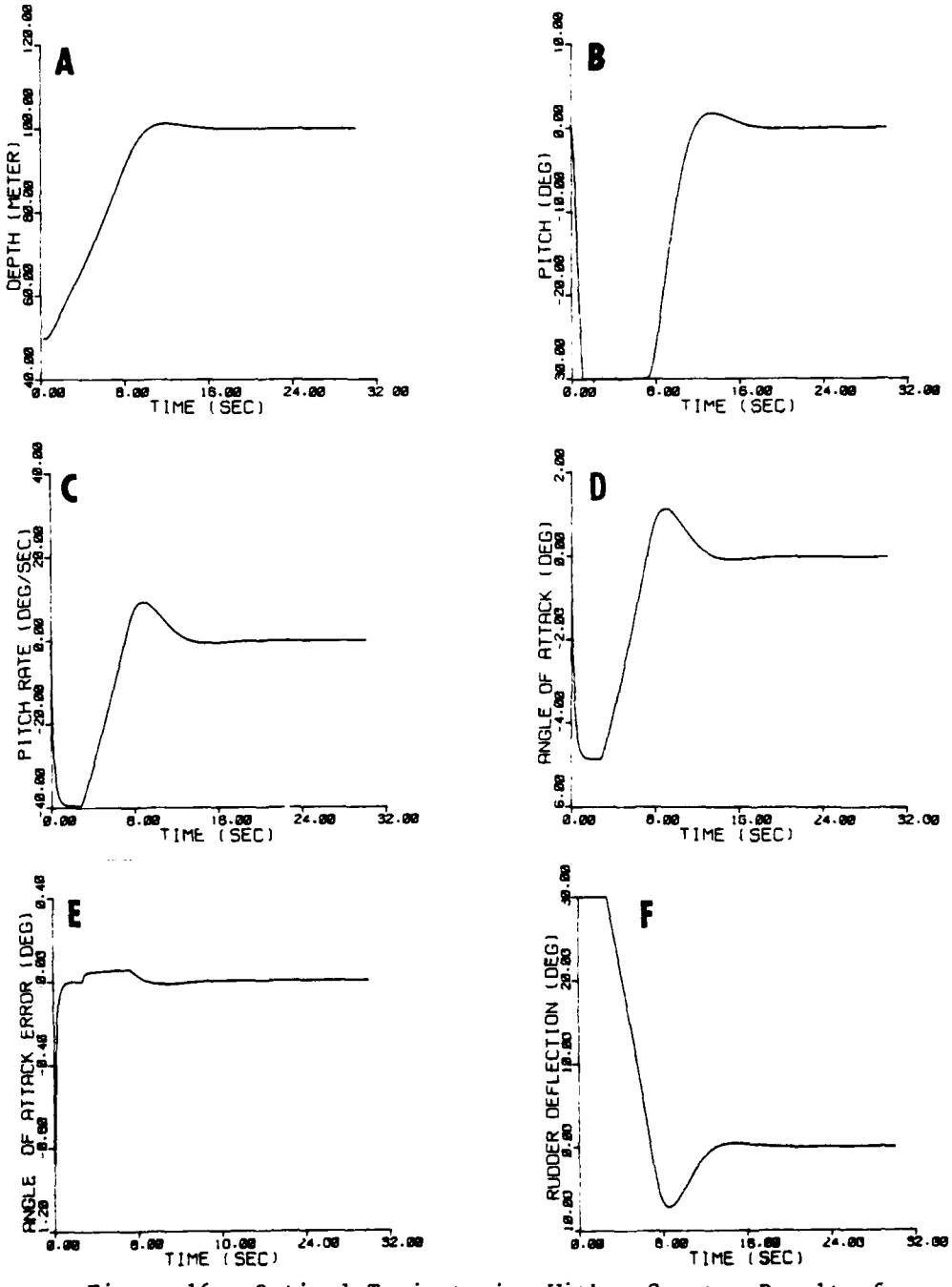


Figure 16. Optimal Trajectories With a Greater Penalty for Depth Errors

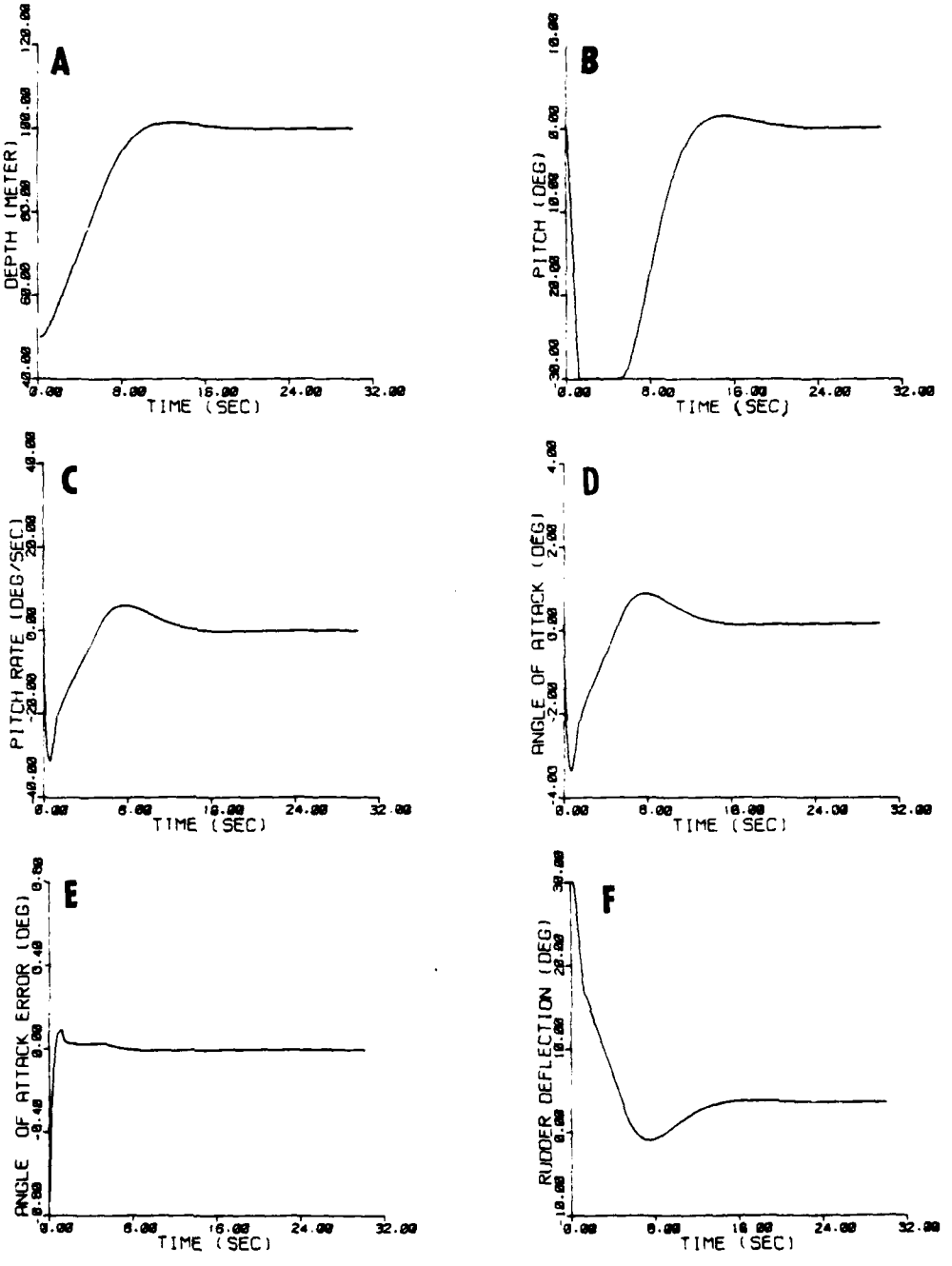


Figure 17. Optimal Trajectories for a Non-neutrally Buoyant Torpedo in a 50-meter Dive at a Constant Speed of 12.5 Meters/sec

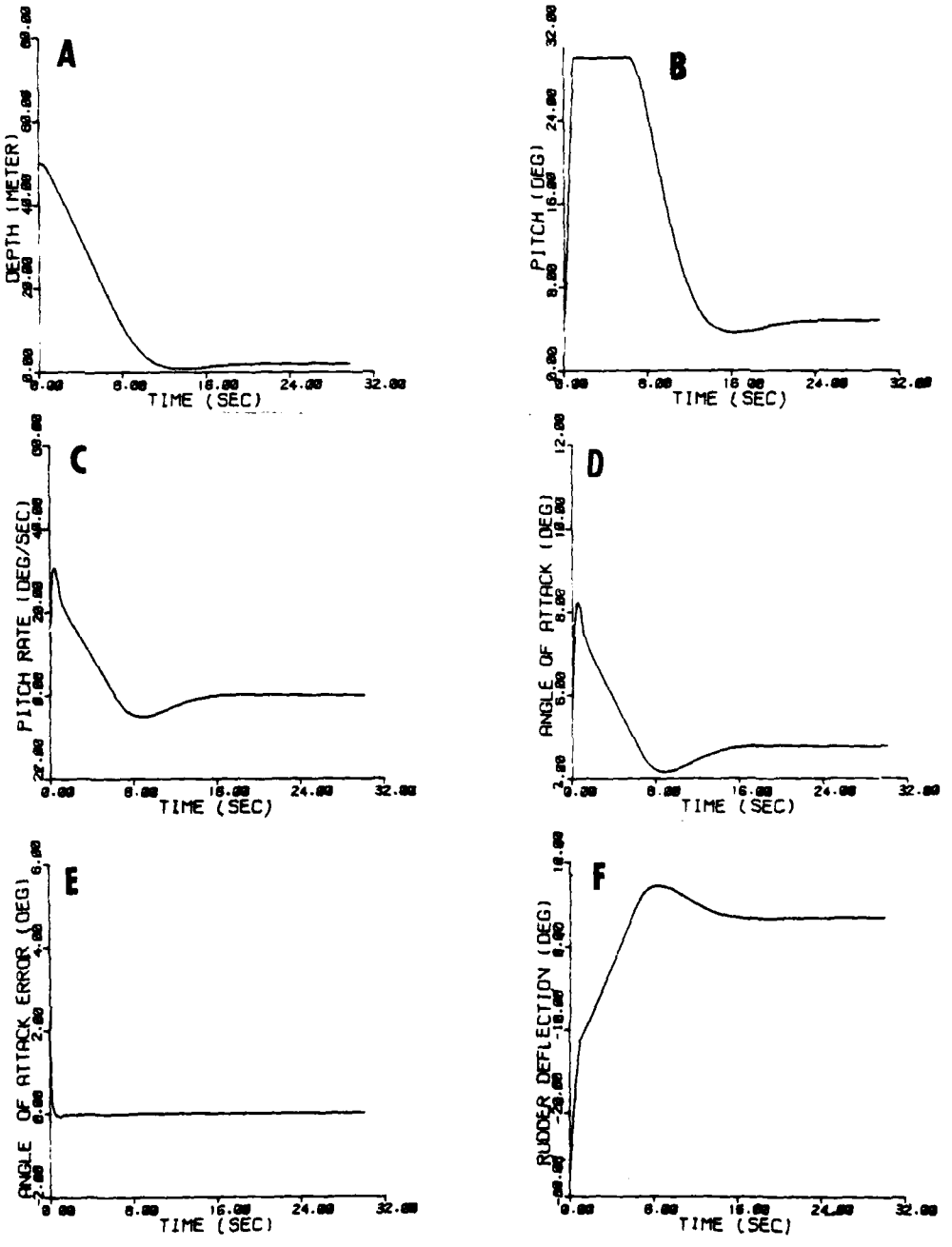


Figure 18. Optimal Trajectories for a Non-neutrally Buoyant Torpedo With Seaway Disturbances in a 48-meter Climb at a Constant Speed of 12.5 Meters/sec

# SECTION V

## SUMMARY, CONCLUSIONS, RECOMMENDATIONS

This report has investigated the feasibility of using modern control theory and Luenberger observer theory in the development of a general controller that is easily adaptable to various underwater vehicles. The closed-loop control scheme was simulated on a digital computer using the hydrodynamic force and moment coefficients of a typical torpedo. Included in the simulations were limitations on torpedo pitch and rudder deflection. The simulations demonstrated that the control scheme performed satisfactorily for the neutrally buoyant model, the non-neutrally buoyant model, and when the torpedo was under the influence of constant seaway disturbances. The effects that the weighting terms in the performance index have on the torpedo trajectory were also shown in the simulations. By varying these terms, suitable torpedo performances were obtained. Changes in simulated torpedo speed were shown to have insignificant effects on the performance of the control scheme.

The control law developed in this report maintains an underwater vehicle on a constant path. In some instances it may be necessary for a torpedo to travel on a time-varying trajectory to a target. The present closed-loop tracking scheme needs to be modified to follow a time-varying reference input. It was also found that the underwater

vehicle can be controlled without feeding back all the states. An investigation into finding a suboptimal control law should be made and the results of this investigation compared against the performance of the optimal control scheme.

## REFERENCES


1. U. DiCaprio and P. P. Wang, "Synthesis of an Optimal Output Regulating System with a Reference Vector," IEEE Transactions on Aerospace and Electronic Systems, Volume AES-7, No. 2, pp. 299-315, March 1971.

2. A. F. Bessacini and A. G. Lindgren, Dynamics and Control of Underwater Vehicles, Technical Report No. 602, Naval Underwater Weapons Research and Engineering Station, Newport, RI, May 1967.

3. D. Leadbeater, "The Application of Classical Control Techniques to the Analysis of a Torpedo Roll Control System," AUWE Technical Note No. 462/72, Admiralty Underwater Weapons Establishment, Portland, England, July 1972.

4. A. G. Lindgren, Dynamics and Control of Submerged Vehicles, Technical Report No. 417-01, Naval Underwater Weapons Research and Engineering Station, Newport, RI, August 1967.

5. T. Noble, Unified Simulation of Marine Vehicles, TP 132, Northrop Corporation, Ventura Division, Newbury Park, CA, April 1969.

6. G. L. Sanders, "Development of the Non-Linear Equation of Motion for Use in Trajectory and Stability and Control Simulation," Technical Memorandum No. 440-12, Pennsylvania State University Institute for Science and Engineering, Applied Research Laboratory, State College, PA, October 1970.

7. D. G. Luenberger, "An Introduction to Observers," IEEE Transactions on Automatic Control, Volume AC-16, No. 6, pp. 596-602, December 1971.

8. L. A. Lopes, Motion Equations for Torpedoes, NOTS 837, Naval Underwater Ordnance Department, China Lake, CA, February 1954.

9. C. T. Chen, Introduction to Linear System Theory, Holt, Rhinehart and Winston, Inc., New York, 1970.

10. F. C. Schweppe, Uncertain Dynamic Systems, Prentice Hall, Inc., Englewood Cliffs, NJ, 1973.

11. M. Athans and P. L. Falb, Optimal Control, McGraw-Hill Book Company, New York, 1966.

# APPENDIX A

## GLOSSARY OF TERMS

### Vehicle Constants

| | | |
|---|---|---|
| m | Vehicle mass | Kg |
| V | Vehicle velocity | meters/sec |
| D | Vehicle diameter | meters |
| W | Vehicle weight | newtons |
| B | Buoyancy | newtons |
| CB | Center of buoyancy | |
| L | Vehicle length | meters |
| CG | Center of gravity | |
| A | Cross-sectional area | $meters^2$ |
| $X_g$ | Distance from CB to CG on X-axis | meters |
| $m_L$ | Longitudinal mass | Kg |
| $m_t$ | Transverse mass | Kg |
| $J_y$ | Moment of inertia about y-axis due to vehicle mass | $Kg\text{-}meter^2$ |
| $V_w$ | Vertical velocity of the water particles | meters/sec |

### Hydrodynamic Coefficients

#### Force Coefficients

$Z_q$ Derivative of normal force component with respect to angular velocity component, q

$Z_\alpha$ Derivative of normal force component with respect to angle of attack, $\alpha$

$Z_w$ Derivative of normal force component with respect to velocity component, w

$Z_{\delta e}$ Derivative of normal force component with respect to elevator angle component, $\delta e$

Moment Coefficients

$M_q$ Derivative of moment component with respect to angular velocity component, q

$M_\alpha$ Derivative of moment component with respect to angle of attack, $\alpha$

$M_w$ Derivative of moment component with respect to vehicle velocity component, w

$M_{\delta e}$ Derivative of moment component with respect to elevator angle component, $\delta e$

# APPENDIX B

## OBSERVABILITY AND CONTROLLABILITY OF WEAPON MODEL

Application of a Luenberger observer and optimal control theory to a time-invariant system described by the state equation

$$\dot{\underline{X}}(t) = A\underline{X}(t)+\underline{b}U(t) \tag{B.1}$$

$$\underline{M}(t) = C\underline{X}(t) \tag{B.2}$$

requires that the system be observable (reference 7) and controllable (reference 1).

Observability Test:

$$\rho(V) = \rho\begin{bmatrix} C \\ CA \\ CA^2 \\ CA^3 \end{bmatrix} = 4$$

The rank of the matrix C is three. The observability of the fourth-order system, (B.1) and (B.2), may be determined (from reference 9 ) by

$$\rho(V_{4-3}) = \rho\begin{bmatrix} C \\ CA \end{bmatrix}$$

$V_{4-3}$ becomes

---

$\rho(\cdot)$ denotes the rank of the matrix

$$V_{4-3} = \begin{bmatrix} 1 & 0 & 0 & 0 \\ 0 & 1 & 0 & 0 \\ 0 & 0 & 1 & 0 \\ 0 & -V & 0 & V \\ 0 & 0 & 1 & 0 \\ 0 & 0 & a_1 & a_2 \end{bmatrix}$$

The rank of $V_{4-3}$ is four; therefore the system is observable. The observability index for this system is two.

Controllability Test:

$$\rho(U) = \rho[\underline{b}\ A\underline{b}\ \overset{2}{A}\underline{b}\ \overset{3}{A}\underline{b}] = 4$$

U becomes

$$U = \begin{bmatrix} 0 & b_2V & U_{13} & U_{14} \\ 0 & b_1 & U_{23} & U_{24} \\ b_1 & U_{32} & U_{33} & U_{34} \\ b_2 & U_{42} & U_{43} & U_{44} \end{bmatrix}$$

where

$$U_{13} = V[(b_1a_3+b_2a_4)-b_1]$$

$$U_{14} = -V[(b_1a_1+b_2a_2)(1+a_3)+a_4(b_1a_3+b_2a_4)]$$

$$U_{23} = b_1a_1+b_2a_2$$

$$U_{24} = a_1(a_1b_1+a_2b_2)+a_2(b_1a_3+b_2a_4)$$

$$U_{32} = b_1a_1+b_2a_2 = U_{23}$$

$$U_{33} = a_1(b_1a_1+b_2a_2)+a_2(b_1a_3+b_2a_4)$$

$$U_{34} = (b_1a_1+b_2a_2)(a_1^2+a_2a_3)+(b_1a_3+b_2a_4)(a_1a_2+a_2a_4)$$

$$U_{42} = b_1a_3+b_2a_4$$

$$U_{43} = a_3(b_1a_1+b_2a_2)+a_4(b_1a_3+b_2a_4)$$

$$U_{44} = (a_3a_1+a_3a_4)(b_1a_1+b_2a_2)+(a_3a_2+a_4^2)(b_1a_3+b_2a_4).$$

Let U be written in a partitioned form as

$$U = \left[\begin{array}{cc:cc} 0 & b_2V & U_{13} & U_{14} \\ 0 & b_1 & U_{23} & U_{24} \\ \hdashline b_1 & U_{23} & U_{33} & U_{34} \\ b_2 & U_{42} & U_{43} & U_{44} \end{array}\right] = \left[\begin{array}{c:c} A & B \\ \hdashline C & D \end{array}\right]$$

where A, B, C, and D are 2×2 matrices. The determinant can be found from the formula (reference 10)

$$|U| = |A - B\,D^{-1}\,C||D|\,. \tag{B.3}$$

Let the $|D| = d$ then (B.3) becomes

$$|U| = |dA - B\,D^{*}\,C| \tag{B.4}$$

where $D^{*}$ is the transpose of the cofactor of the matrix D.

The determinant of the matrix D is given by

$$d = |D| = U_{33}\,U_{44} - U_{34}\,U_{43}\,, \tag{B.5}$$

and the transpose of the matrix D becomes

$$D^* = \begin{bmatrix} U_{44} & -U_{34} \\ -U_{43} & U_{33} \end{bmatrix}. \tag{B.6}$$

Substituting equation (B.5) and (B.6) into equation (B.4), the determinant of the matrix U is written as

$$|U| = \begin{vmatrix} -(U_{13}U_{44}-U_{14}U_{43})b_1 & db_2V-(U_{13}U_{44}-U_{14}U_{43})U_{32} \\ -(U_{14}U_{33}-U_{13}U_{34})b_2 & -(U_{14}U_{33}-U_{13}U_{34})U_{42} \\ -(U_{23}U_{44}-U_{24}U_{43})b_1 & db_1-(U_{23}U_{44}-U_{24}U_{43})U_{32} \\ -(U_{24}U_{33}-U_{23}U_{34})b_2 & -(U_{24}U_{33}-U_{23}U_{34})U_{42} \end{vmatrix}. \tag{B.7}$$

The determinant of the matrix U becomes

$$\begin{aligned} |U| = {} & -[(U_{13}U_{44}-U_{14}U_{43})b_1+(U_{14}U_{33}-U_{13}U_{34})b_2][db_1-(U_{23}U_{44}-U_{24}U_{43})U_{32} \\ & -(U_{24}U_{33}-U_{23}U_{34})U_{42}] + [db_2V-(U_{13}U_{44}-U_{14}U_{43})U_{32}-(U_{14}U_{33}-U_{13}U_{34})U_{42}] \\ & [(U_{23}U_{44}-U_{24}U_{43})b_1+(U_{24}U_{33}-U_{23}U_{34})b_2]. \end{aligned} \tag{B.8}$$

The determinant, equation (B.8), cannot be evaluated until the elements of the A matrix and $\underline{b}$ vector are defined for a specific application. Therefore, before an optimal control law can be formulated for the underwater vehicle state variable model, equation (B.8) must be evaluated for the specific vehicle constants and hydrodynamic coefficients.

# APPENDIX C

## STATE TRANSITION MATRIX

The state transition matrix is found by taking an inverse Laplace transform of the resolvent matrix. The resolvent matrix for a time-invariant system described by the state equations

$$\dot{\underline{X}}(t) = A\underline{X}(t)+BU(t) \tag{C.1}$$

$$\underline{M}(t) = \underline{C}\underline{X}(t) \tag{C.2}$$

is given by

$$\Phi(S) = [SI-A]^{-1}.$$

The matrix [SI-A] is written in a partitioned form as

$$[SI-A] = \left[\begin{array}{cc:cc} S & V & 0 & -V \\ 0 & S & -1 & 0 \\ \hdashline 0 & 0 & S-a_1 & -a_2 \\ 0 & 0 & -a_3 & S-a_4 \end{array}\right] = \left[\begin{array}{c:c} a & b \\ \hdashline \phi & c \end{array}\right] \tag{C.3}$$

where a, b, and c are 2×2 matrices and $\phi$ denotes a 2×2 null matrix. The inverse is found by multiplying equation (C.3) by a matrix such that the product yields the identity matrix. Let

$$\left[\begin{array}{c:c} a & b \\ \hdashline \phi & c \end{array}\right] \left[\begin{array}{c:c} D & E \\ \hdashline F & G \end{array}\right] = \left[\begin{array}{c:c} I & \phi \\ \hdashline \phi & I \end{array}\right] \tag{C.4}$$

where D, E, F, and G are 2×2 matrices and I is a 2×2 identity matrix. The resolvent matrix is given by

$$\Phi(S) = \left[\begin{array}{c|c} D & E \\ \hline F & G \end{array}\right]. \tag{C.5}$$

Multiplying out equation (C.4) yields

$$\left[\begin{array}{c|c} aD+bF & aE+bG \\ \hline cF & cG \end{array}\right] = \left[\begin{array}{c|c} I & \phi \\ \hline \phi & I \end{array}\right].$$

Equating terms and solving for D, E, F, and G yields

$$F = \phi$$

$$G = c^{-1} = \frac{\begin{bmatrix} S-a_4 & a_2 \\ a_3 & S-a_1 \end{bmatrix}}{(S-a_4)(S-a_1)-a_2a_3}$$

$$D = a^{-1} = \begin{bmatrix} 1/S & -V/S^2 \\ 0 & 1/S \end{bmatrix}$$

and

$$E = -a^{-1}\, b\, c^{-1} = -\frac{\begin{bmatrix} (S-a_4)\dfrac{V}{S^2} - \dfrac{a_3V}{S} & \dfrac{a_2V}{S^2} - \dfrac{(S-a_1)V}{S} \\ \dfrac{-(S-a_4)}{S} & \dfrac{-a_2}{S} \end{bmatrix}}{[(S-a_4)(S-a_1) - a_2\, a_3}.$$

From equation (C.5), the resolvent matrix is given by

$$\Phi(S) = \begin{bmatrix} 1/S & -V/S^2 & \dfrac{V(a_3-1)S+a_4V}{S^2[(S-W)(S-Z)]} & \dfrac{VS^2-a_1VS-a_2V}{S^2(S-W)(S-Z)} \\ 0 & 1/S & \dfrac{(S-a_4)}{S[(S-W)(S-Z)]} & \dfrac{a_2}{S[(S-W)(S-Z)]} \\ 0 & 0 & \dfrac{(S-a_4)}{(S-W)(S-Z)} & \dfrac{a_2}{(S-W)(S-Z)} \\ 0 & 0 & \dfrac{a_3}{(S-W)(S-Z)} & \dfrac{(S-a_1)}{(S-W)(S-Z)} \end{bmatrix} \quad (C.6)$$

where

$$W = \frac{a_1+a_4+\sqrt{(a_1+a_4)^2+4(a_2a_3-a_1a_4)}}{2}$$

and

$$Z = \frac{a_1+a_4-\sqrt{(a_1+a_4)^2+4(a_2a_3-a_1a_4)}}{2}.$$

The inverse Laplace transform of equation (C.6) yields the state transition matrix of the form

$$\Phi(t) = \begin{bmatrix} 1 & -Vt & A_1t+A_2+A_3\epsilon^{Wt}+A_4\epsilon^{Zt} & E_1t+E_2+E_3\epsilon^{Wt}+E_4\epsilon^{Zt} \\ 0 & 1 & B_1t+B_2\epsilon^{Wt}+B_3\epsilon^{Zt} & F_1t+F_2\epsilon^{Wt}+F_3\epsilon^{Zt} \\ 0 & 0 & C_1\epsilon^{Wt}+C_2\epsilon^{Zt} & G_1\epsilon^{Wt}+G_2\epsilon^{Zt} \\ 0 & 0 & D_1\epsilon^{Wt}+D_2\epsilon^{Zt} & H_1\epsilon^{Wt}+H_2\epsilon^{Zt} \end{bmatrix} \quad (C.7)$$

where the coefficients are found by performing a partial fraction expansion of the terms in the resolvent matrix, equation (C.6). The partial fraction expansion of the term $\Phi_{13}(S)$ is

$$\frac{V(a_3-1)S+a_4V}{S^2(S-W)(S-Z)} = \frac{A_1}{S^2} + \frac{A_2}{S} + \frac{A_3}{S-W} + \frac{A_4}{S-Z} .$$

$$A_1 = \left.\frac{V(a_3-1)S+a_4V}{(S-W)(S-Z)}\right|_{S=0} = \frac{a_4V}{WZ}$$

$$A_2 = \frac{d}{dS}\left[\frac{V(a_3-1)S+a_4V}{(S-W)(S-Z)}\right]\Bigg|_{S=0} = -\left.\frac{(S-W)(S-Z)V(a_3-1)-[V(a_4-1)S+a_4V][2S-W-Z]}{(S-W)^2(S-Z)^2}\right|_{S=0}$$

$$A_2 = \frac{WZV(a_3-1)+a_4V(W+Z)}{W^2Z^2}$$

$$A_3 = \left.\frac{V(a_3-1)S+a_4V}{S^2(S-Z)}\right|_{S=W} = \frac{V(a_3-1)W+a_4V}{W^2(W-Z)}$$

$$A_4 = \left.\frac{V(a_3-1)S+a_4V}{S^2(S-W)}\right|_{S=Z} = \frac{V(a_3-1)Z+a_4V}{Z^2(Z-W)}$$

The partial fraction expansion of the term $\Phi_{23}(S)$ is

$$\frac{(S-a_4)}{S(S-W)(S-Z)} = \frac{B_1}{S} + \frac{B_2}{S-W} + \frac{B_3}{S-Z}$$

$$B_1 = \left.\frac{(S-a_4)}{(S-W)(S-Z)}\right|_{S=0} = -\frac{a_4}{WZ}$$

$$B_2 = \left.\frac{(S-a_4)}{S(S-Z)}\right|_{S=W} = \frac{W-a_4}{(W-Z)W}$$

$$B_3 = \left.\frac{(S-a_4)}{S(S-W)}\right|_{S=Z} = \frac{Z-a_4}{(Z-W)Z}\,.$$

The partial fraction expansion of the term $\Phi_{33}(S)$ is

$$\frac{S-a_4}{(S-W)(S-Z)} = \frac{C_1}{S-W} + \frac{C_2}{S-Z}$$

$$C_1 = \left.\frac{(S-a_4)}{(S-Z)}\right|_{S=W} = \frac{W-a_4}{W-Z}$$

$$C_2 = \left.\frac{(S-a_4)}{(S-W)}\right|_{S=Z} = \frac{Z-a_4}{Z-W}\,.$$

The partial fraction expansion of the term $\Phi_{43}(S)$ is

$$\frac{a_3}{(S-W)(S-Z)} = \frac{D_1}{S-W} + \frac{D_2}{S-Z}$$

$$D_1 = \left.\frac{a_3}{S-Z}\right|_{S=W} = \frac{a_3}{W-Z}$$

$$D_2 = \left.\frac{a_3}{S-W}\right|_{S=Z} = \frac{a_3}{Z-W} .$$

The partial fraction of the term $\Phi_{14}(S)$ is

$$\frac{VS^2-a_1VS-a_2V}{S^2(S-W)(S-Z)} = \frac{E_1}{S^2} + \frac{E_2}{S} + \frac{E_3}{S-W} + \frac{E_4}{S-Z}$$

$$E_1 = \left.\frac{VS^2-a_1VS-a_2V}{(S-W)(S-Z)}\right|_{S=0} = \frac{-a_2V}{WZ}$$

$$E_2 = \left.\frac{d}{dS}\left[\frac{VS^2-a_1VS-a_2V}{(S-W)(S-Z)}\right]\right|_{S=0}$$

$$= \left.\frac{(S-W)(S-Z)[2VS-a_1V]-[VS^2-a_1VS-a_2V](2S-W-Z)}{(S-W)(S-Z)}\right|_{S=0}$$

$$E_2 = \frac{-WZa_1V-a_2V(W+Z)}{W^2Z^2}$$

$$E_3 = \left.\frac{VS^2-a_1VS-a_2V}{S^2(S-Z)}\right|_{S=W} = \frac{VW^2-a_1VW-a_2V}{W^2(W-Z)}$$

$$E_4 = \left.\frac{VS^2-a_1VS-a_2V}{S^2(S-W)}\right|_{S=Z} = \frac{VZ^2-a_1VZ-a_2V}{Z^2(Z-W)} .$$

The partial fraction expansion of the term $\Phi_{24}(S)$ is

$$\frac{a_2}{S(S-W)(S-Z)} = \frac{F_1}{S} + \frac{F_2}{S-W} + \frac{F_3}{S-Z}$$

$$F_1 = \left.\frac{a_2}{(S-W)(S-Z)}\right|_{S=0} = \frac{a_2}{WZ}$$

$$F_2 = \left.\frac{a_2}{S(S-Z)}\right|_{S=W} = \frac{a_2}{W(W-Z)}$$

$$F_3 = \left.\frac{a_2}{S(S-W)}\right|_{S=Z} = \frac{a_2}{Z(Z-W)}.$$

The partial fraction expansion of the term $\Phi_{34}(S)$ is

$$\frac{a_2}{(S-W)(S-Z)} = \frac{G_1}{S-W} + \frac{G_2}{S-Z}$$

$$G_1 = \left.\frac{a_2}{S-Z}\right|_{S=W} = \frac{a_2}{W-Z}$$

$$G_2 = \left.\frac{a_2}{S-W}\right|_{S=Z} = \frac{a_2}{Z-W}.$$

The partial fraction expansion of the term $\Phi_{44}(S)$ is

$$\frac{S-a_1}{(S-W)(S-Z)} = \frac{H_1}{S-W} + \frac{H_2}{SZ}$$

$$H_1 = \left.\frac{S-a_1}{S-Z}\right|_{S=W} = \frac{W-a_1}{W-Z}$$

$$H_2 = \left.\frac{S-a_1}{S-W}\right|_{S=Z} = \frac{Z-a_1}{Z-W} .$$

# APPENDIX D

## TRANSFER FUNCTION OF THE OBSERVER

The state variable model is given by

$$\begin{bmatrix} \dot{X}_1(t) \\ \dot{X}_2(t) \\ \dot{X}_3(t) \\ X_4(t) \end{bmatrix} = \begin{bmatrix} 0 & -V & 0 & V \\ 0 & 0 & 1 & 0 \\ 0 & 0 & a_1 & a_2 \\ 0 & 0 & a_3 & a_4 \end{bmatrix} \begin{bmatrix} X_1(t) \\ X_2(t) \\ X_3(t) \\ X_4(t) \end{bmatrix} + \begin{bmatrix} 0 \\ 0 \\ b_1 \\ b_2 \end{bmatrix} U(t) \tag{D.1}$$

$$\begin{bmatrix} m_1(t) \\ m_2(t) \\ m_3(t) \end{bmatrix} = \begin{bmatrix} 1 & 0 & 0 & 0 \\ 0 & 1 & 0 & 0 \\ 0 & 0 & 1 & 0 \end{bmatrix} \begin{bmatrix} X_1(t) \\ X_2(t) \\ X_3(t) \\ X_4(t) \end{bmatrix} \tag{D.2}$$

and the reduced-order observer is written as

$$\dot{W}(t) = -\sigma W(t) + \left[a_3 - \frac{(\sigma+a_4)(\sigma+a_1)}{a_2}\right] m_3(t) + \left[b_2 - \frac{b_1(\sigma+a_4)}{a_2}\right] U(t). \tag{D.3}$$

A signal flow graph of the model given by equations (D.1), (D.2), and (D.3) is shown in figure D-1. The signal flow graph in figure D-1 can be simplified by calculating the open-loop transfer functions from the equation

$$\underline{G}(S) = C\, \Phi(S) \underline{b}$$

where

$$C = \begin{bmatrix} 1 & 0 & 0 & 0 \\ 0 & 1 & 0 & 0 \\ 0 & 0 & 1 & 0 \end{bmatrix}$$

$$\underline{b} = \begin{bmatrix} 0 \\ 0 \\ b_1 \\ b_2 \end{bmatrix}$$

and $\Phi(S)$ is the resolvent matrix in appendix C. Using the above equation,

$$\begin{bmatrix} G_1(S) \\ G_2(S) \\ G_3(S) \end{bmatrix} = \begin{bmatrix} \dfrac{b_2V\,S^2 + (b_1a_3V - b_1V - b_2a_1V)S + b_1Va_4 - b_2a_2V}{S^2(S-W)(S-Z)} \\ \dfrac{b_1S - b_1a_4 + b_2a_2}{S(S-W)(S-Z)} \\ \dfrac{b_1S - b_1a_4 + b_2a_2}{(S-W)(S-Z)} \end{bmatrix}.$$

Let

$$f_1 = G_1(S) = \frac{m_1(S)}{U(S)}$$

$$f_2 = G_2(S) = \frac{m_2(S)}{U(S)}$$

and

$$f_3 = G_3(S) = \frac{m_3(S)}{U(S)} = sf_2,$$

then the signal flow graph is modified to the signal flow graph of figure 2.

Mason's Formula and figure 2 are used to find the transfer function, $\frac{X_4(S)}{U(S)}$.

Loops:

$$L_1 = \frac{a_4}{S} \qquad L_2 = \frac{a_2 a_3}{S^2} \qquad \text{and } L_3 = \frac{a_1}{S}$$

$$\Delta = 1-(L_1+L_2+L_3)+L_1L_3$$

$$\Delta = \frac{S^2-(a_4+a_1)S-a_2a_3+a_4a_1}{S^2}.$$

Forward Paths:

$$G_1 = \frac{b_2}{S} \qquad \Delta_1 = \frac{S-a_1}{S}$$

and

$$G_2 = \frac{b_1 a_3}{S^2} \qquad \Delta_2 = 1$$

Transfer Function:

$$\frac{X_4(S)}{U(S)} = \frac{G_1\Delta_1+G_2\Delta_2}{\Delta} = \frac{b_2S-b_2a_1+b_1a_3}{S^2-(a_4+a_1)S-a_2a_3+a_4a_1} . \qquad (D.4)$$

Figure D-2 is used to find the transfer function, $\frac{\hat{Z}(S)}{U(S)}$.

Loop:

$$L_1 = -\frac{\sigma}{S}$$

$$\Delta = \frac{S+\sigma}{S}$$

Forward Paths:

$$G_1 = \frac{b_2}{S} - \frac{b_1(\sigma+a_4)}{a_2S} \qquad \Delta_1 = 1$$

$$G_2 = \frac{\sigma+a_4}{a_2} f_3 \qquad \Delta_2 = \frac{S+\sigma}{S}$$

and

$$G_3 = \{a_3 - \frac{a_1(\sigma+a_4)}{a_2} - \frac{\sigma(\sigma+a_4)}{a_2}\} \frac{f_3}{S} \qquad \Delta_3 = 1$$

Transfer Function:

$$\frac{\hat{Z}(S)}{U(S)} = \frac{\dfrac{b_2}{S}\,\dfrac{b_1(\sigma+a_4)}{a_2 S}\,\dfrac{\sigma+a_4}{a_2}\,f_3\,\dfrac{(S+\sigma)}{S} + \left[a_3\,\dfrac{-a_1(\sigma+a_4)}{a_2}\,\dfrac{-\sigma(\sigma+a_4)}{a_2}\right]\dfrac{f_3}{S}}{\dfrac{S+\sigma}{S}}$$

which reduces to

$$\frac{\hat{Z}(S)}{U(S)} = \frac{b_2\,a_2 - b_1(\sigma+a_4) + [\sigma S + a_4 S - \sigma a_1 - a_4 a_1 + a_3 a_2]\,f_3}{a_2(S+\sigma)}.$$

Substituting for $f_3$ and cancelling similar terms yields

$$\frac{\hat{Z}(S)}{U(S)} = \frac{a_2(S+\sigma)\,[b_2 S - b_2 a_1 + b_1 a_3]}{[S^2 - (a_4+a_1)S - a_2 a_3 + a_4 a_1]\,a_2\,(S+\sigma)}$$

$$\frac{\hat{Z}(S)}{U(S)} = \frac{b_2 S - b_2 a_1 + b_1 a_3}{S^2 - (a_4+a_1)S - a_2 a_3 + a_4 a_1}. \qquad (D.5)$$

Comparing equations (D.4) and (D.5) shows that

$$\frac{X_4(S)}{U(S)} = \frac{\hat{Z}(S)}{U(S)}.$$

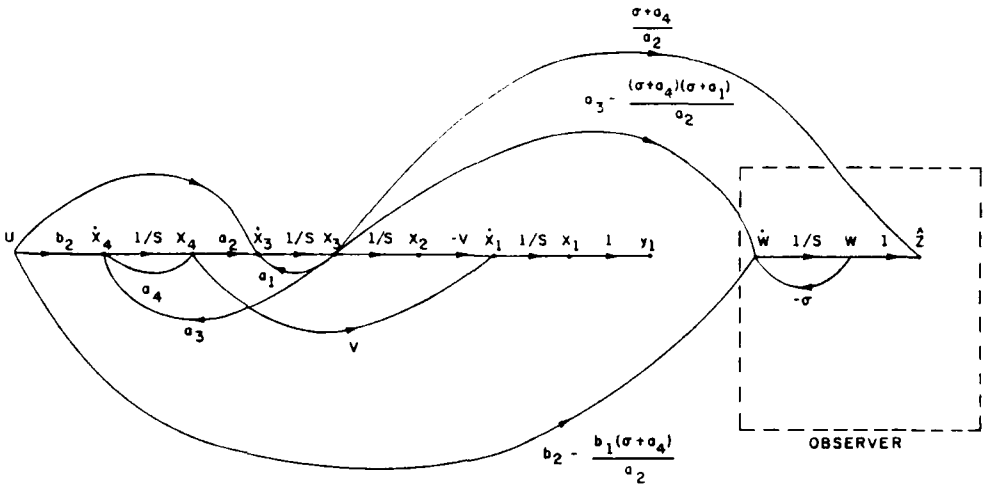


Figure D-1. Signal Flow Graph of the State Variable Model with the Observer

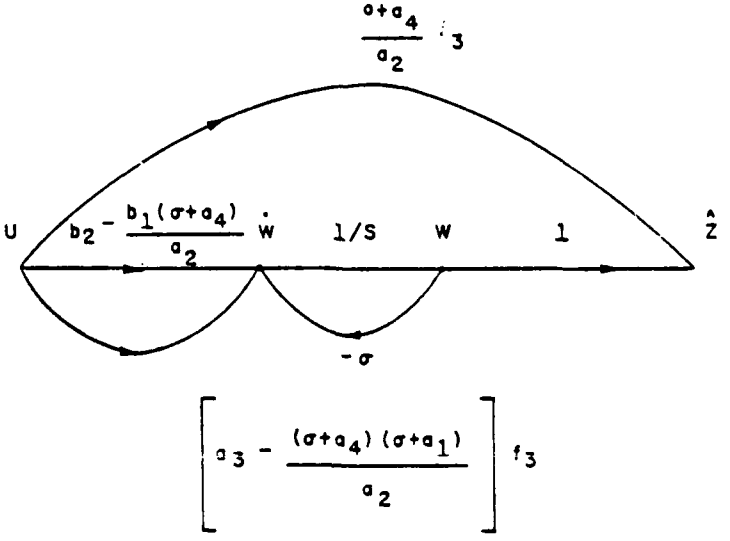


Figure D-2. Reduced Signal Flow Graph of the State Variable Model with the Observer

# INITIAL DISTRIBUTION LIST

| Addresee | No. of Copies |
|---|---|
| COMTRALANT | 2 |
| COMTRAPAC | 2 |
| COMFLTRAGRU PEARL | 2 |
| COMFLTRAGRU WSTPC | 2 |
| COMFLTRAGRU GTMO | 2 |
| OUSDR&E (Research and Advanced Technology, W. J. Perry) | 2 |
| CNR (ONR-100; ONR-431, J. Smith) | 2 |
| CNO (OP-02, OP-35, OP-39) | 3 |
| CNM (MAT-08T1) | 1 |
| NSWC, White Oak | 1 |
| NAVSEA (SEA-06; SEA-06D; SEA-06R; SEA-63R; SEA-63R-13; SEA-632X; PMS-393, R. Bowers) | 7 |
| NOSC | 1 |
| NCSL | 1 |
| CHESNAVFACENGCOM | 1 |
| FLTASWTRACENLANT | 5 |
| NAVPGSCOL | 1 |
| DDC | 12 |